Table 4-1. Existing *Zic* Mutant Mice

Gene/Allele	Type	Lethality?[a]	Reference
Zic1^{-}	null	perinatal[b]	(Aruga, Minowa et al. 1998)
Zic2^{kd}	hypomorph	perinatal	(Nagai, Aruga et al. 2000)
Zic2^{ku}	null	mid embryonic	(Elms, Siggers et al. 2003)
Zic2^{m1Nisw}	hypomorph	perinatal	(Zhang and Niswander 2013)
Zic3^{Bn}	spontaneous null mutation	early[c]	(Carrel, Purandare et al. 2000; Klootwijk, Franke et al. 2000)
Zic3^{-}	null	varies[d]	(Purandare, Ware et al. 2002)
Zic3^{flox}	conditional	none	(Sutherland, Wang et al. 2013)
Zic4^{-}	null	none	(Grinberg, Northrup et al. 2004; Blank, Grinberg et al. 2011)
Zic5^{tm1Jaru}	null	postnatal[e]	(Inoue, Hatayama et al. 2004)
Zic5^{tm1Sia}	null	perinatal	(Furushima, Murata et al. 2005)
Zic1^{-}; *Zic4*$^{-}$	null	postnatal	(Grinberg, Northrup et al. 2004; Blank, Grinberg et al. 2011)

[a] mid-embryonic (E13.5), perinatal (E17.5 to P1), postnatal (P1 to P21)
[b] 50% die before P1, all die by P21
[c] embryonic, but no exact age specified
[d] no definitive time point (death occurs prior to E10.5 and into adults)
[e] some die by P3, all die by P60

development (Barald and Kelley 2004; Bok, Bronner-Fraser et al. 2005; Choo 2007) and which is a critical source of SHH and WNT signals to the developing inner ear (Klootwijk, Franke et al. 2000; Nagai, Aruga et al. 2000; Riccomagno, Martinu et al. 2002; Inoue, Hatayama et al. 2004; Riccomagno, Takada et al. 2005). Because the neural tube is a source of both SHH and WNT signaling, and these signaling pathways are critical for inner ear development, the interpretation of data from these *Zic* mutant mice is not straightforward. The question is still unanswered: Are *Zic* genes ***directly*** involved in inner ear development, or is altered ear formation secondary to neural tube defects caused by the loss of *Zic* genes (Riccomagno, Martinu et al. 2002; Riccomagno, Takada et al. 2005). Further, no data exists showing with which genes ZIC proteins interact in the hindbrain, otic epithelium, and periotic mesenchyme, so attempts at determining the mechanism of *Zic* function in inner ear development are limited to speculating

which genes might be affected based on the morphological phenotype. The following discussion details ways to model *Zic* gene loss in both mouse and chick and how to determine with which genes ZICs interact. Using this information, experiments can be proposed to investigate the mechanism of *Zic* gene function during inner ear development.

4.2. Modeling *Zic* Mutations in Mouse and Chick

As described above, the current *Zic* mutant mice are poorly suited to investigating the role of *Zic* genes in inner ear development. Lethality, defects in the neural tube, a major signaling center during inner ear development, and the inability to selectively and specifically isolate *Zic* gene loss to specific regions of the developing inner ear are all major issues that need to be addressed.

Conditional *Zic* Knockout Mice

Using the Cre-Lox system, the loss of each *Zic* gene could be more carefully controlled, thereby avoiding or significantly delaying the lethality associated with the global loss of these genes. Careful selection of the specific Cre-driver mouse line could also restrict the loss of each *Zic* gene to a specific tissue (e.g., neural tube, periotic mesenchyme), enabling the analysis of *Zic* gene function in isolated regions of the developing inner ear. If more precise timing is required, an inducible Cre-driver line could be used, further restricting the loss of *Zic* genes in time, as well as space.

To date, *Zic3* is the only *Zic* gene with a conditional (floxed) allele

Table 4-2. Floxed Alleles of *Zic* Genes Being Developed

Gene	Project	Status
Zic1	KOMP-CSD	Design Completed
Zic2	KOMP-CSD	Vector Design In Progress
Zic4	EUCOMM	VEGA Annotation Requested
Zic5	EUCOMM	Vector Construction In Progress

(Sutherland, Wang et al. 2013). Currently, laboratories are developing floxed alleles of the other *Zic* genes, though many are still early in the process (Table 4-2; EUCOMM 2013). Once mice have been generated with these floxed alleles, they would be bred to $Tbx18^{Cre}$ (mesenchyme; Trowe, Shah et al. 2010) or $Hoxa3^{Cre}$ (rhombomeres 5 and 6; Macatee, Hammond et al. 2003) mice to generate mice with complete loss of *Zic* expression in either the periotic mesenchyme or the neural tube adjacent to the inner ear (the analysis of these mice will be described in a later section). After generating single conditional mutants, compound conditional *Zic* mutants would be created. Initially, *Zic2*/*Zic5* and *Zic2*/*Zic3*/*Zic5* compound mutants will be generated, as these *Zic* genes have overlapping expression patterns within the developing inner ear and therefore have the highest possibility of functional redundancy/compensation (Chervenak, Hakim et al. 2013). A $Zic1^{flox}$/$Zic4^{flox}$ compound mutant would not be necessary to generate, as the *Zic1*/*Zic4* compound mutant (Grinberg, Northrup et al. 2004; Blank, Grinberg et al. 2011) is viable up to post-natal stages and does not appear to have defects in inner ear development, as shown by our paint-fills. Generation of a conditional mouse with complete loss of all 5 *Zic* genes in either the mesenchyme or the neural tube would also be informative and could address at which stages of ear development function of the *Zic* genes is critical.

Knockdown of *Zic* Genes in Chick Embryos Using *In Ovo* Electroporation

As a complimentary approach to selectively knocking out *Zic* genes using the Cre-Lox system in mice, *in ovo* electroporation of chicken embryos could be used. *In ovo* electroporation has been used to overexpress or knockdown the expression of genes in a variety of tissues in the chick, including the neural tube, limb mesoderm, dermomyotome, and somites (Krull 2004; Nakamura, Katahira et al. 2004; Scaal, Gros et al. 2004; Das, Van Hateren et al. 2006). The advantage of these experiments is that the targeted area can be tightly controlled by limiting the size of the electrodes, the strength of the electrical field, and the location of where the plasmid DNA (containing the cDNA of the gene to be over-expressed or the RNA sequence targeting the gene to be knocked down) is injected. These experiments used to be limited to those tissues located near a natural reservoir for the DNA solution, such as the lumen of the neural tube, but new techniques using DNA-soaked beads allow for the localization of the plasmid DNA to nearly any tissue (Simkin, McKeown et al. 2009).

For these experiments, multiple micro RNA (miRNA) sequences to target *Zic1-4* could be designed and cloned into the pRFPRNAiC vector (Das, Van Hateren et al. 2006). Previously, experiments were designed to knockdown *Zic1* and *Zic2* in the otocyst in chick embryos. As part of these experiments, a plasmid with a miRNA sequence targeting GFP (pRFPRNAiC-GFP) was co-electroporated with a plasmid expressing GFP (pCAX-EGFP) into the otic cup of a HH stage 10 chick embryo to see if the plasmid worked in the otic cup/otocyst

(Figure 4-2). The pRFPRNAiC-GFP plasmid effectively knocked down expression of GFP in the otocyst, demonstrating that this plasmid worked in the inner ear in chick. miRNA sequences to target *Zic1* (2 sequences) and *Zic2* (2 sequences) were designed and tested in the dorsal neural tube, but none of these resulted in effective knockdown of either *Zic1* or *Zic2* in the neural tube (unpublished results). Additionally, expression analysis of the *Zic* genes in the chick inner ear (Chervenak, Hakim et al. 2013) showed that none of the *Zic* genes is expressed in the otic epithelium, so the previous experimental design (knocking down *Zic* genes in the otic epithelium) was abandoned.

Just as for the *Zic* riboprobes, the miRNA sequences for each *Zic* gene would be designed to target regions of low similarity among the different *Zic* genes (i.e. outside of the ZF, ZOC, and ZF-NC domains; refer to Figure 2-3). Initially, each target sequence would be tested individually, but eventually two different target sequences directed against the same *Zic* gene could be cloned into a single RNAi plasmid to increase knockdown efficiency. To test each miRNA target sequence, the left dorsal neural tube of HH stage 18 (*Zic1-3*) or HH stage 24 (*Zic4*) chick embryos could be electroporated with the miRNA plasmid. These specific stages would be used because older embryos (HH stage 17-20) survive better after electroporation and because significant expression of *Zic4* is not detected in the neural tube until HH stage 24, compared to HH stage 18 for *Zic1-3* (Chervenak, Hakim et al. 2013). After electroporation, the embryos

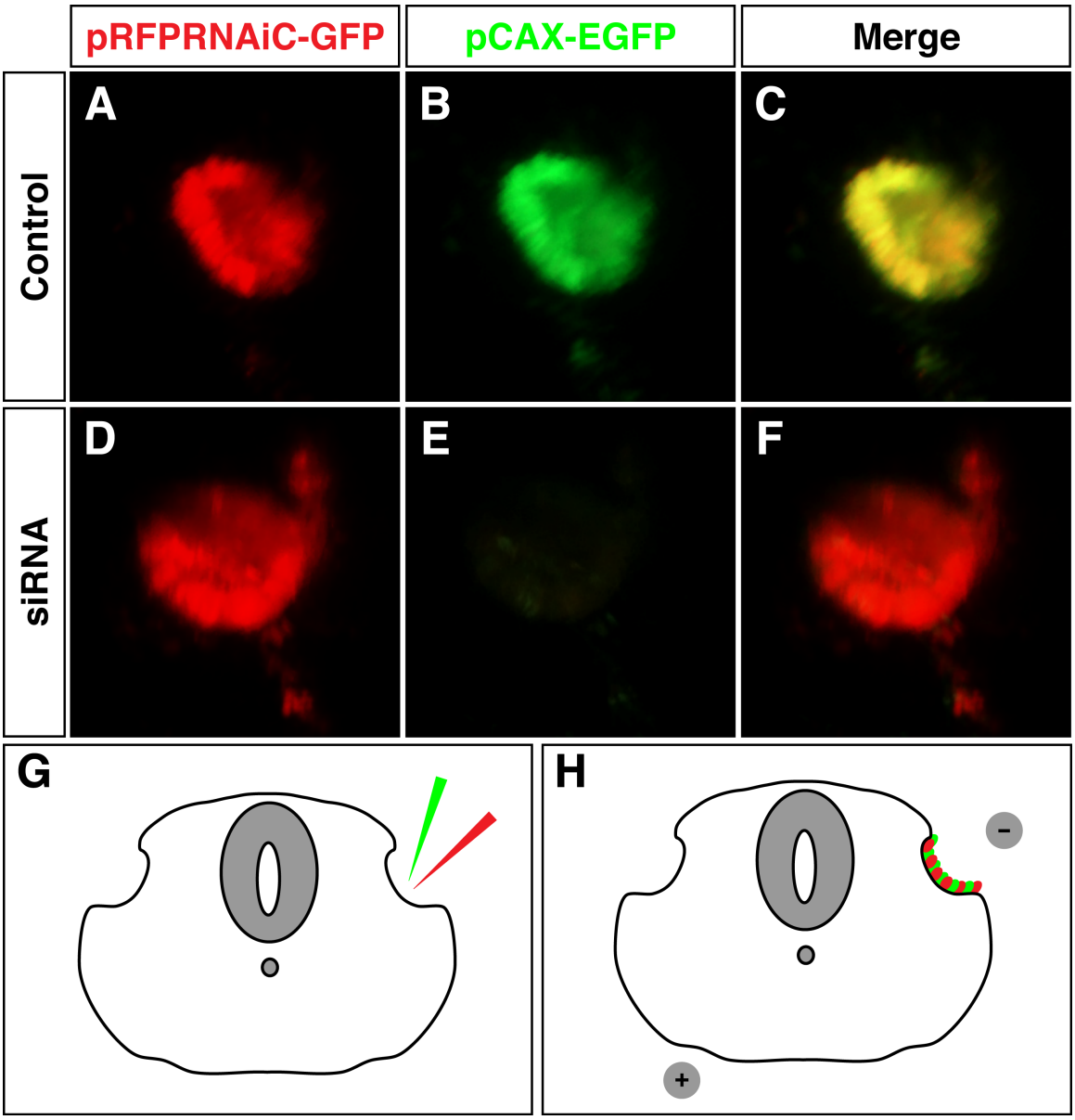

Figure 4-1. Validation of siRNA Knockdown System in Chick Inner Ear. Otocysts from chick embryos at HH stage 13 were injected with a combination of either pRFPRNAiC and pCAX-EGFP (A-C; "control") or pRFPRNAiC-GFP and pCAX-EGFP (D-F; "siRNA") to test this siRNA system in the chick inner ear. Otic cups successfully electroporated with the control combination of plasmids were both RFP+ (A) and GFP+ (B). Otic cups successfully electroporated with the siRNA combination of plasmids were RFP+ (D) and GFP- (E), indicating that the RNAi target sequence directed against GFP mRNA reduced or eliminated GFP mRNA, leading to undetectable expression of GFP protein (compare panel B to panel E). (G, H) Experimental design schematic. Plasmids (pRFPRNAiC or pRFPRNAiC-GFP, red; pCAX-EGFP, green) were co-injected into the otocyst (G), then electrodes were positioned as in (H) to target the plasmid DNA to cells in the otic cup.

would be allowed to develop for an additional 24-36 hours before being collected, fixed, and sectioned. *In situ* hybridization would then be performed using a probe for the *Zic* gene that was targeted. Probes for the other *Zic* genes could also be used to demonstrate the specificity of the knockdown; if the knockdown was successful, then there would be a drastic reduction in the number of *Zic*-expressing cells in the left dorsal neural tube (electroporated) compared to the right dorsal neural tube (unelectroporated) as shown by *in situ* hybridization. Antibodies to the specific ZIC protein whose mRNA was targeted in the siRNA electroporation experiment would also be used to demonstrate that reduced levels of mRNA result in reduced protein levels: RFP+ cells (electroporated) in the left dorsal neural tube should be negative for the ZIC protein being targeted, and the ZIC protein level should be lower in the left dorsal neural tube compared to the right dorsal neural tube.

Another factor needing to be addressed is the length of time that *Zic* knockdown can be achieved from the standard pRFPRNAiC plasmid. For testing the miRNA target sequences, the plasmid only needs to be active for 24-36 hours, which is within the time range used in experiments using this plasmid (Das, Van Hateren et al. 2006). In the actual experiments, embryos would be electroporated at HH stage 10 (~E2) and analyzed as late as HH stage 32 (~E7.5), so expression of the miRNA must be maintained the entire time. The simplest read-out for plasmid activity is RFP expression, so initially embryos would be electroporated in the left dorsal neural tube at HH stage 10, allowed to develop until HH stage 32, and then whole embryos viewed under a dissecting

microscope by UV illumination through an RFP filter to see if RFP+ cells are still present in the electroporated side of the neural tube. If they are, then embryos would be collected and processed as described above, using riboprobes (*in situ* hybridization) and antibodies (immunofluorescence) to assess knockdown at both the mRNA and protein levels. If RFP+ cells were not seen, then the replication competent avian splice (RCAS) vector would be used instead, as it was shown to not only remain active but also to spread to new cells over the course of longer experiments (Das, Van Hateren et al. 2006).

Once the *Zic* miRNA plasmids have been created and tested, the dorsal neural tube adjacent to the otic cup or the periotic mesenchyme surrounding the otic cup of HH stage 10 chick embryos will be electroporated with the miRNA plasmids to knockdown each of the *Zic* genes (Figure 4-2). For the neural tube electroporations, plasmid DNA would be injected into the lumen of the neural tube and the electrodes positioned to target the left dorsal neural tube (Figure 4-2A). Since no easily-accessible lumen exists to hold the plasmid DNA for the periotic mesenchyme electroporations, beads would be soaked with the plasmid DNA (Simkin, McKeown et al. 2009), carefully implanted into the mesenchyme, and then electroporated in at least two different directions to ensure targeting of multiple regions of the periotic mesenchyme (Figure 4-2B). The exact area for bead implantation, as well as the number and direction of electroporations required to target the majority of the periotic mesenchyme would need to be determined, as well as the tolerance of embryos to bead implantation and multiple electroporations.

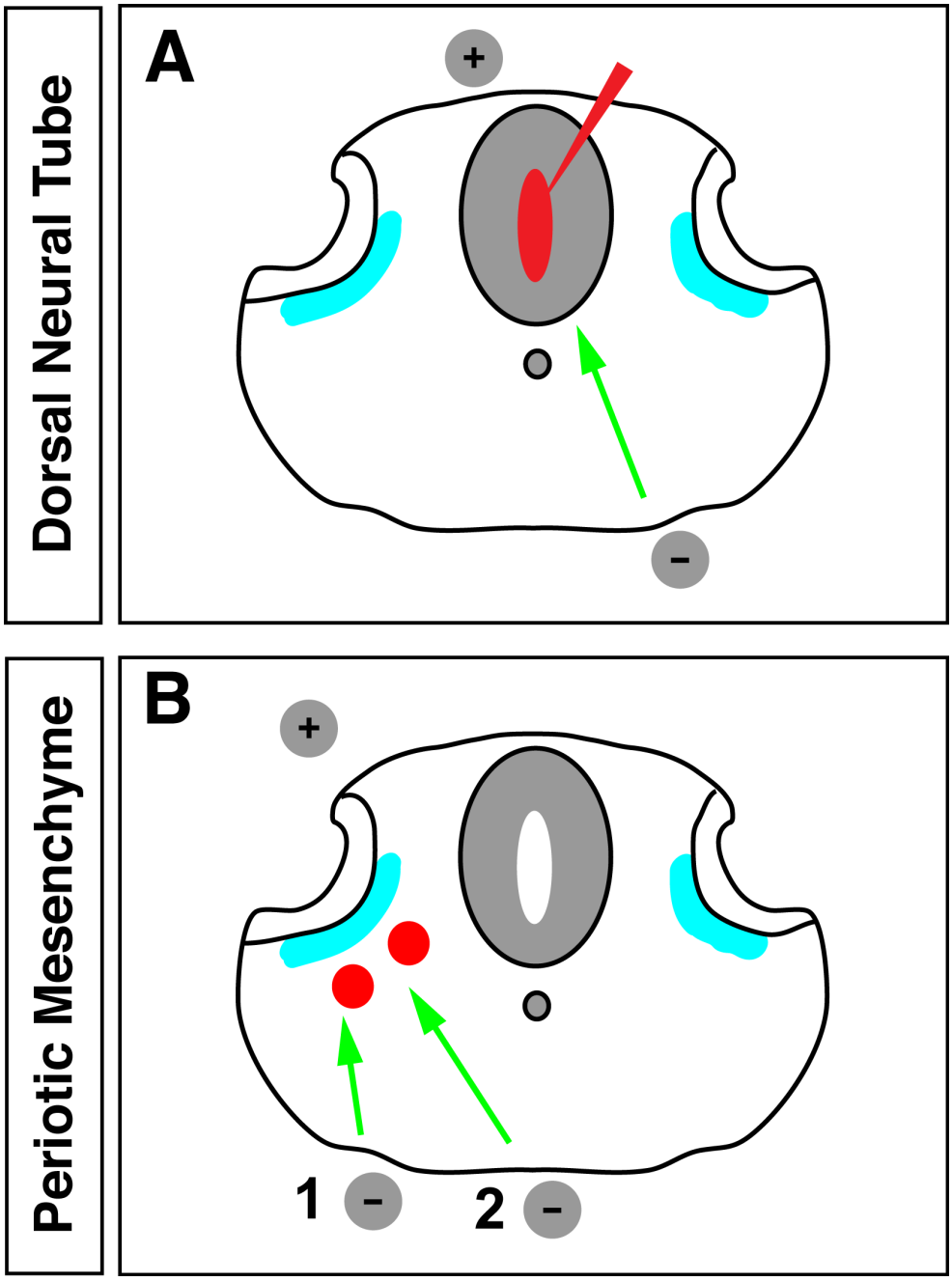

Figure 4-2. Electroporation Strategies to Target Dorsal Neural Tube and Periotic Mesenchyme. (A) Plasmid DNA (red) is injected into the lumen of the neural tube and then electrodes are positioned so that the current flows in the direction of the left dorsal neural tube, resulting in targeting of cells in the left dorsal neural tube. (B) Plasmid DNA-soaked beads (red) are implanted underneath the periotic mesenchyme and then electrodes are placed at position 1, the embryo is electroporated, and then the electrodes moved to position 2 and electroporated again so that a large extent of the periotic mesenchyme is targeted. Green arrows illustrate direction of current flow, and thus point to location being targeted.

In an alternative approach, antisense oligonucleotide morpholinos targeting the *Zic* genes could be electroporated directly into the developing chick inner ear. We successfully used this strategy to examine the role of the *DAN* gene in inner ear development in the chick embryo (Gerlach-Bank, Cleveland et al. 2004) and have also used this strategy to examine the role of other genes involved in both nervous system and inner ear development and distinguish them from one another in the zebrafish (Holmes, Wyatt et al. 2011; Shen, Thompson et al. 2012).

4.3. Inner Ear Morphology of Conditional *Zic* Mouse Mutants and Electroporated Chick Embryos

After generating the conditional *Zic* mouse mutants and chick embryos with reduced *Zic* gene expression through any of these strategies, embryos would be collected at different time points and their inner ears paint-filled to analyze changes in inner ear morphology. Mouse embryos (mutants and wild type littermates) would be collected at E11.5, E12.5, E13.5, and E16.5, while chick embryos (electroporated and mock electroporated) would be collected at HH stages 18, 24, 32, and 35 (~E3, E4.5, E7, and E9). After dissection and fixation, inner ears would be filled with a paint solution as described previously (Kiernan 2006). Comparisons would be made between inner ears from wild type or mock electroporated embryos and those from *Zic* conditional knockouts or electroporated embryos. The results from these experiments will show which *Zic* genes are most critical for inner ear development and could be used to guide and

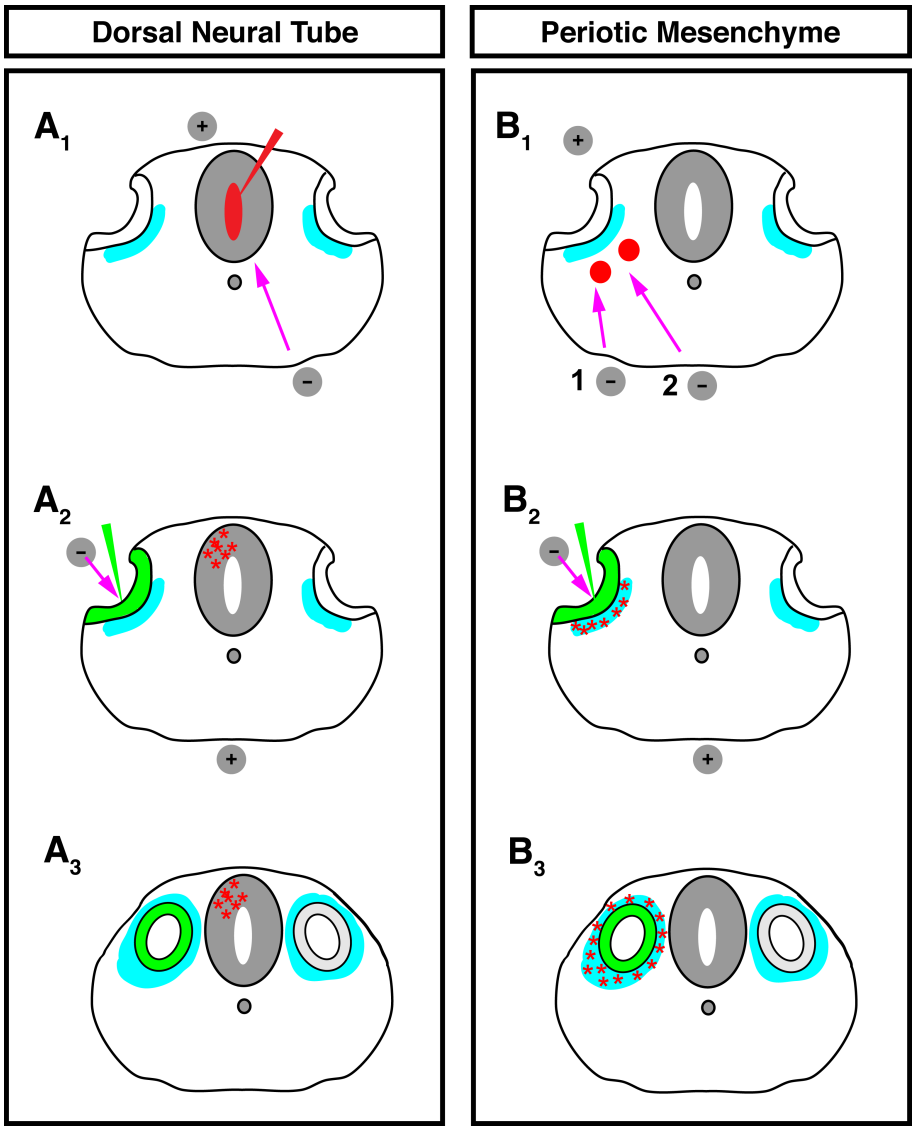

Figure 4-3. Electroporation Scheme For Live Imaging of Inner Ear Morphogenesis in Chick Embryos After *Zic* Knock-Down. (A) Electroporation of dorsal neural tube with *Zic* siRNA plasmid (A1), followed by electroporation of the otic cup with RCAS-BA-EGFP (A2) to observe otic epithelium morphogenesis after otic cup closure in inner ears with one of the *Zic* genes knocked-down in the neural tube (A3). (B) Electroporation of periotic mesenchyme with *Zic* siRNA plasmid (B1), followed by electroporation of the otic cup with EGFP-tagged beta-actin (B2) to observe otic epithelium morphogenesis after otic cup closure in inner ears with one of the *Zic* genes knocked-down in the periotic mesenchyme (B3). Red indicates siRNA plasmid injection/bead placement (A1, B1) and red asterisks indicate cells electroporated with *Zic* siRNA or control siRNA plasmids (A2, B2). Green indicates site of injection of RCAS-BA-EGFP (A2, B2) or beta-actin/EGFP-tagged otic epithelial cells (A3, B3). Blue area adjacent to otic epithelium marks the periotic mesenchyme. Magenta arrows (A1, A2, B1, B2) indicate direction of current and thus points to cells that will be electroporated.

prioritize future experiments.

4.4. Live-Imaging of Inner Ear Morphogenesis in Chick Embryos

Once the *Zic* genes that most affect inner ear development in chick have been identified, we would attempt live cell imaging to visualize the changes in inner ear morphogenesis when these *Zic* genes are knocked-down. Two separate electroporation schemes would be employed: in the first scheme, we would electroporate the *Zic* siRNA plasmids into the dorsal neural tube and electroporate the proviral RCASBP(B) plasmid containing a coding sequence for β-actin-EGFP (RCAS-BA-EGFP) into the otic cup at HH stage 13 (Figure 4-3A; Bird, Daudet et al. 2010), and in the second scheme we would electroporate the *Zic* siRNA plasmids into the periotic mesenchyme and RCAS-BA-EGFP into the otic cup at HH stage 13 (Figure 4-3B). Then, 16-24 hours after electroporating (~HH stage 18) we would set-up for live confocal imaging of the inner ear in an intact chick embryo to observe morphogenesis of the inner ear as it occurs and compare it to the morphogenesis of embryos electroporated with the control siRNA plasmid and RCAS-BA-EGFP. One benefit of the periotic mesenchyme elctroporations would be the ability to have both the otic epithelium and periotic mesenchyme labeled with different fluorescent proteins (periotic mesenchyme in red, otic epithelium in green) so that interactions between the periotic mesenchyme and otic epithelium could be observed. What happens to the periotic mesenchyme when *Zic* genes are knocked down? What happens to proliferation in the periotic mesenchyme when Zic genes are knocked down?

Under normal conditions, how does the periotic mesenchyme move in relation to the otic epithelium? These same observations could be made for the electroporations in which the dorsal neural tube was targeted, except an additional electroporation would need to be performed using a third fluorescent protein to label the periotic mesenchyme.

A possible complication to this approach would be the depth of imaging required, as the otocyst at HH stage 18 is between 150 and 200μm, which would be difficult to image completely. As inner ear morphogenesis proceeds, portions of the ear would thin along the medio-lateral axis before widening again, and along the dorso-ventral axis, tremendous lengthening occurs. To control for this, separate movies could be made of the inner ear along its dorso-ventral axis. Another imaging scheme would be to take thick transverse sections through the inner ear at HH stage 18, place them in imaging chambers with minimal media, and use a confocal equipped with an environmental chamber to keep the sections close to physiological conditions, allowing them to survive through the imaging period (Bird, Daudet et al. 2010).

4.5. Identifying Transcriptional Targets of *Zic* Genes

Very little is known about downstream targets of *Zic* genes, and what little is known is limited to their roles in regions other than the inner ear. Gain and loss of function studies, primarily in fish and frog, and analysis of mouse mutants has identified a few genes in which expression changes have been documented in response to changes in *Zic* expression (Brewster, Lee et al. 1998; Aruga 2004).

However, the results to date indicate that these genes (including *Wnt3a*, *NeuroD*, *Atoh1*, and *Cyclin D1*, among others) are downstream of *Zic* genes, and not necessarily direct transcriptional targets (see Table 4 in Aruga 2004). Previous *in vitro* studies have identified ZIC binding sequences in the promoters of a handful of genes and have demonstrated that these are direct transcriptional targets of *Zic* genes (see Table 1C in Merzdorf 2007). No experiments to date have looked for direct transcriptional targets of *Zic* genes in whole embryos or isolated tissues.

ChIP-chip to Identify *Zic* Transcriptional Targets in the Inner Ear

As a first step to identifying genes that are direct transcriptional targets of *Zic* genes in the inner ear, chromatin immunoprecipitation followed by hybridization to a mouse promoter microarray (ChIP-chip) would be employed. Wild type mice would be collected at E8.5 (otic placode), E9.0 (otic cup), E9.5 (early otocyst), E10.5 (late otocyst), E11.5, E12.5, E13.5, E15.5, and E17.5 (progressive stages of inner ear morphogenesis) and the inner ear regions dissected. Tissues (otic placode/otic epithelium, periotic mesenchyme, and neural tube) would be microdissected and pooled from multiple embryos, then prepared for chromatin immunoprecipitation (ChIP). After ChIP using antibodies to ZIC1, ZIC2, ZIC3, ZIC4, or ZIC5, the resulting DNA would be hybridized to a mouse promoter microarray (Agilent Technologies). These experiments would identify which promoters each of the ZIC proteins occupies, as well as where and when, during inner ear development.

4.6. Changes in Gene Expression in *Zic* Mutants

Microarray analysis would be used to identify genes whose expression changes in response to loss of each of the *Zic* genes in the inner ear. As for the ChIP-chip experiments, tissues (otic placode/otic epithelium, periotic mesenchyme, neural tube) would be microdissected from mouse embryos between E8.5 and E17.5. However, in addition to tissues from wild type mice, tissues would also be collected from the conditional *Zic* mutant mice (described in section 4.2.1). RNA would be extracted from the tissues, amplified and labeled (RNA from wild type tissue labeled with one fluorophore, RNA from mutant tissue labeled with a different fluorophore), and then applied to a mouse cDNA microarray such that comparisons are made between wild type and mutant tissues from the same region (otic placode/otic epithelium, periotic mesenchyme, neural tube) at the same time point. Results from the microarray experiments could then be sorted into logical arrangements (e.g., by signaling pathway, type of gene, ear developmental process) to guide further hypotheses.

The results from the microarray experiments could then be compared to the ChIP-chip data to differentiate between direct and indirect targets of ZIC proteins. That is, if the expression of gene “X” decreased in the periotic mesenchyme in the $Zic1^{flox/flox};Tbx18^{Cre}$ and gene “X” was identified in the ChIP-chip experiment, then gene “X” is a direct transcriptional target of *Zic1* in the periotic mesenchyme. If gene “X” was not identified in the ChIP-chip experiment, then gene “X” is not a direct transcriptional target of *Zic1* but instead lies downstream of *Zic1*. Then, if gene “X” is a direct transcriptional target of gene

"Y", and from the experiments gene "Y" was shown to be a direct transcriptional target of *Zic1*, then a possible transcriptional pathway can be assembled (*Zic1*→ Gene "Y"→ Gene "X"). Thus, combining the microarray data and the ChIP-chip data with current knowledge about signaling pathways involved in inner ear development would enable the placement of the *Zic* genes within these signaling pathways and possibly identify signaling networks with the *Zic* genes acting as factors that integrate multiple signaling pathways into networks.

4.7. Validation of Microarray Experiments

Once genes in which the expression increases or decreases significantly in response to loss of each of the *Zic* genes are identified, these results would need to be validated by *in situ* hybridization in conditional *Zic* mutant mouse embryos. Since there would likely be a large number of genes to validate, the experiments would be prioritized starting with those genes shown to be direct transcriptional targets of ZIC proteins. After that, genes whose downstream targets are best characterized would be given the highest priority. Once the findings of the microarray experiments had been validated, the hypothesized signaling pathways/networks could be tested. Previously described mouse mutants might be reexamined for changes in *Zic* gene expression, further solidifying the role of *Zic* genes in those specific signaling pathways/networks. Additionally, in mouse mutants with inner ear defects, *Zic* genes that are direct targets of those genes could be added back through the introduction of a bacterial artificial chromosome containing the *Zic* gene under control of a different promoter to express the ZIC

protein. If the added *Zic* gene rescues the inner ear defects, then this further strengthens the order of those genes in a signaling pathway affecting inner ear development.

4.8. Conclusions

The *Zic* genes play a role in inner ear development, as they are expressed in cells of the periotic mesenchyme and dorsal neural tube adjacent to the inner ear during development in both mouse and chick (Chervenak, Hakim et al. 2013), and inner ears from *Zic2*$^{kd/kd}$ and *Zic2*$^{Ku/Ku}$ mice have a range of morphological defects (Chervenak, Gerlach-Bank et al., manuscript in preparation). However, limited knowledge about what genes ZIC proteins interact with both in the entire organism, as well as specifically in the inner ear, makes it difficult to determine what next steps to take. Further complicating matters is that true *Zic* null mice often die during embryonic development or perinatally from a variety of neural defects, making analysis of inner ear development difficult. The experiments outlined here would provide new *Zic* mouse models, as well as a complimentary *Zic* loss of function model in chick embryos, identify direct transcriptional targets of *Zic* genes in the inner ear, and identify genes further downstream of the *Zic* genes during inner ear development. Combining these new tools and knowledge, better hypotheses could be made regarding the role of *Zic* genes in inner ear development in both mouse and chick that could be tested in complementary animal models more amenable to the genetic manipulations and live imaging experiments proposed above for chick and mouse.

Appendix

Additional Data

A.1. Results and Discussion

Effects of *Zic2* Loss on Signaling Pathways Involved in Inner Ear Development

FGF Signaling

FGFs, especially *Fgf3* and *Fgf10* in the mouse, are critical for the initial specification of the otic placode, as mice lacking both *Fgf3* and *Fgf10* fail to form otic vesicles (Wright and Mansour 2003). In $Zic2^{Ku/Ku}$ mutants, otic vesicles form and look normal compared to otic vesicles from wild type and heterozygous mice (Figure 3-4, compare otic vesicles in panel C' with those in panels A' and B'). In cross-section, the overall size and shape of the otic vesicles from $Zic2^{Ku/Ku}$ mutants are similar to wild type and heterozygous mice, with the only appreciable difference being that the otic vesicles in most of the $Zic2^{Ku/Ku}$ mutants are positioned at a ~45-80^{o} angle from the normal dorsal-ventral (vertical) orientation seen in heterozygotes and wild type embryos. The extent of this positional shift depends on the extent of the failure of the neural tube to close, and varies both among mutants (e.g., compare otocysts from embryos #1, #2, and #3 in Supplemental Figure 9) and even within the same mutant embryo (compare

otocysts from different sections of the same mutant embryos in Figures A-8 [embryo #2], A-22 [embryo #2], and Supplemental Figures 4 [embryo #2] and 10). Since the otic vesicles formed and looked normal, we concluded that the initial specification of the otic placode and subsequent morphogenetic events were relatively unaffected. It is possible that either *Fgf3* or *Fgf10* expression was affected, as otic vesicle formation does occur in mice with a loss of either *Fgf3* or *Fgf10* (Wright and Mansour 2003). Due to the unavailability of mutant embryos at E8-E9, the age when the otic placode is specified, we cannot rule out this possibility.

We examined the expression of *Fgf3* (Figure A-1) and *Fgf10* (Figure A-2) in the otic region of *Zic2*$^{+/+}$, *Zic2*$^{Ku/+}$, and *Zic2*$^{Ku/Ku}$ embryos at E9.5 and E10.5. *Fgf3* expression was found in the neural tube and the medial wall of the branchial arch in all embryos at E9.5, though the positioning of the branchial arch (ba; yellow arrows) is altered in the *Zic2*$^{Ku/Ku}$ embryos (Figure A-1). At E10.5, *Fgf3* expression was detected in all embryos. In the *Zic2*$^{Ku/Ku}$ embryos, there was a cluster of *Fgf3*+ cells adjacent to the medial wall of the otic epithelium that was also seen in the wild type embryos, though the cluster of cells was much smaller (blue asterisks in Figure A-1). Without further replicates, it is difficult to determine if the size difference in this cluster of cells represents a real difference between mutant and wild type embryos, as this experiment was only performed once and some sections were lost in this region of the ear in the wild type and heterozygous embryos. *Fgf10* expression at E9.5 was difficult to detect in these samples, so we cannot begin to speculate about differences in expression

among the *Zic2*$^{+/+}$, *Zic2*$^{Ku/+}$, and *Zic2*$^{Ku/Ku}$ mice. Expression of *Fgf10* was more readily demonstrated at E10.5 and was observed in all embryos in the ventral and ventral-medial wall of the otocyst and in the mesenchyme immediately adjacent to this region (blue asterisks in Figure A-2). As with the *Fgf3* experiments, we were limited to analysis of a single mutant embryo, so further experiments are needed before we can draw any definitive conclusions. In addition, since there are many FGF proteins, it may be better to use antibodies to detect pERK expression as a readout of FGF pathway activation.

BMP Signaling

To determine if BMP signaling was affected in the inner ears from *Zic2*$^{Ku/Ku}$ mice, we performed immunofluorescence experiments using a phospho-Smad-1/5/8 antibody on sections through the inner ear region at E9.5 (Figure A-3), E11.5 (Figure A-4), and E12.5 (Figure A-5). Phospho-Smad-1/5/8 is a read-out of BMP pathway activation, so changes in the expression of phospho-Smad-1/5/8 would indicate that BMP signaling had been altered. We were only able to examine one or two mutants at each age, and the data for these mutants was variable and of poor quality, making interpretation difficult. We also examined the expression pattern of one of the BMP ligands, *Bmp4* (Figure A-6). Expression at both E9.5 and E10.5 varied widely in sections from *Zic2*$^{+/+}$, *Zic2*$^{Ku/+}$, and *Zic2*$^{Ku/Ku}$ mice, so we could not determine a consistent expression pattern for any of the three genotypes. Due to the small numbers of replicates and wide variations in the

quality of the data, we were unable to draw any conclusions about changes in BMP pathway activation in the inner ears from the *Zic2*$^{Ku/Ku}$ mutants.

SHH Signaling

Another key signaling pathway involved in inner ear development is the SHH pathway. *Shh* secreted from the notochord and floor plate of the ventral neural tube signals to the mesenchyme and the otic epithelium where it positively regulates the expression of the SHH pathway genes *Ptch1* and *Gli1*. *Shh* also either positively or negatively regulates the expression of a number of downstream genes involved in inner ear development, as well as opposes WNT signals from the dorsal neural tube (Riccomagno, Martinu et al. 2002; Riccomagno, Takada et al. 2005).

We first used *in situ* hybridization to look at the expression of *Ptch1* as a readout of SHH pathway activation (Figures A-7 through A-11). In wild type mice at both E9.5 and E10.5, *Ptch1* expression extends in all directions from the notochord and ventral neural tube, the source of SHH ligand (Figure A-7A, A-7D). In the inner ear region, *Ptch1* expression was found in the ventral two-thirds of the neural tube, in the ventro-medial otic epithelium, and in the mesenchyme directly below the *Ptch1*-expressing portion of the otic epithelium (Figure A-7A, A-7D). Both heterozygotes and mutants exhibited a similar expression pattern (*cf*. Figures A-7B, A-7E, Figures A-7C, A-7F and Figures A-7A, A-7D), indicating that SHH signaling at these ages appears to be unaffected by the partial or total loss of *Zic2*. Starting at E11.5 the expression pattern of *Ptch1* changes slightly as

morphogenesis of the inner ear proceeds (Figure A-7G, H, I). In *Zic2*$^{+/+}$, *Zic2*$^{Ku/+}$, and *Zic2*$^{Ku/Ku}$ mice, expression was maintained in the ventral portion of the neural tube, but expanded to a larger portion of the otic epithelium as the epithelium expanded ventro-medially (and closer to the source of SHH ligand) due to the emergence of the cochlear duct. *Ptch1* expression in the mesenchyme was primarily limited to cells near the midline of the embryo, but also extended to cells located dorso-laterally between the neural tube and the developing ear. By E12.5 (Figure 3-10J, K, L), *Ptch1* expression appeared to become restricted to cells near the lumen of the ventral neural tube and to cells in portions of the otic epithelium closest to the midline. In the mesenchyme, expression was not detected, except in the *Zic2*$^{Ku/Ku}$ mutant. However, our *in situs* gave variable expression patterns at E12.5 for *Ptch1* in the *Zic2*$^{Ku/Ku}$ mutants, ranging from undetectable to seemingly much higher than that detected in either wild type or heterozygous mice. It is possible that this variability in the expression of *Ptch1* in the *Zic2*$^{Ku/Ku}$ mutants is correlated with the severity of the neural tube closure defect. Again, due to variability in the strength of the signal from the *in situs* and the low number of replicates, we cannot make any definitive statements about the status of SHH pathway activation in the *Zic2*$^{Ku/Ku}$ mutants. We also examined the expression of *Gli1* as another readout of SHH pathway activation, though our analysis was limited to one embryo per genotype (*Zic2*$^{+/+}$, *Zic2*$^{Ku/+}$, *Zic2*$^{Ku/Ku}$) at E9.5 (Figure A-12). As for the *Ptch1 in situs*, the results of these experiments were variable, preventing us from drawing any conclusions from this data.

To further investigate the SHH pathway, we analyzed the expression of the SHH pathway ligand, *Shh*, at E9.5 and E10.5 (Figures A-13 and A-14). In *Zic2*$^{+/+}$, *Zic2*$^{Ku/+}$, and *Zic2*$^{Ku/Ku}$ embryos, *Shh* expression was detected in the floor plate of the ventral neural tube, as well as in the notochord, at both E9.5 and E10.5, consistent with findings from the original characterization of the *Zic2 Kumba* mutant (Elms, Siggers et al. 2003). The notochord in some sections is missing, although we observed this in samples from all genotypes. This is most likely due to the notochord peeling off of some sections during the *in situs*, as the loose arrangement of cells in the mesenchyme along the midline does not allow cells in this region to adhere as tightly to the microscope slides. Overall, we did not observe any changes in *Shh* expression in the *Zic2*$^{Ku/Ku}$ mice; however, further replicates are needed.

WNT Signaling

The WNT signaling pathway is another of the major pathways involved in inner ear development. *Wnt1* and *Wnt3a* from the dorsal neural tube signal to the otic epithelium and periotic mesenchyme, positively regulating the expression of the WNT pathway gene *Axin2*, as well as either positively or negatively regulating the expression of a number of downstream genes involved in inner ear development, and opposes SHH signals from the ventral neural tube (Riccomagno, Martinu et al. 2002; Riccomagno, Takada et al. 2005). We first examined the expression of *Axin2* as a readout of WNT signaling to see if pathway activation was altered in the *Zic2* mutants (Figures A-15 through A-19). At E9.5, *Axin2* expression was

found in the dorsal neural tube and in the mesenchyme between the neural tube and the otic epithelium, as well as in the mesenchyme directly under the ventral region of the otic epithelium in both wild type (Figure A-15A, Figure A-16) and heterozygous mice (Figure A-15B, Figure A-16). In the one mutant with an open neural tube, *Axin2* expression was weakly detected in the same regions as in wild type and heterozygous mice (*cf*. Figure A-15C and Figure A-15A, A-15B). However in a *Zic2* mutant with no neural tube closure defect in the region of the developing inner ear, the expression pattern of *Axin2* was indistinguishable from that of wild type and heterozygous mice (embryo #2, Figure A-16). The expression pattern of *Axin2* at E10.5 mirrored that at E9.5, though the distance between the region of expression in the dorsal neural tube and the otic epithelium was much greater in the $Zic2^{Ku/Ku}$ mutants (cf. Figure A-15F and Figure A-15D, A-15E; Figure A-17). By E11.5, the expression of *Axin2* remained in the dorsal neural tube (although expression is weakly detected in the mutants), but mesenchymal expression became restricted to the dorso-medial region between the neural tube and the otic epithelium in the anterior half of the developing inner ear, though this expression appeared to be slightly increased in the mutants (Figure A-15G-I; Figure A-18). *Axin2* expression was weakly detected in the dorsal neural tube and completely absent in the mesenchyme in $Zic2^{+/+}$, $Zic2^{Ku/+}$, and $Zic2^{Ku/Ku}$ embryos at E12.5 (Figure A-19).

To further investigate the WNT pathway, we analyzed the expression of the WNT pathway ligands, *Wnt1* and *Wnt3a*, at E9.5 and E10.5 (Figures A-20 through A-23). In $Zic2^{+/+}$, $Zic2^{Ku/+}$, and $Zic2^{Ku/Ku}$ embryos at E9.5, *Wnt1*

expression was found in the dorsal-most portion of the neural tube, with no changes in expression seen among the different genotypes (Figure A-20). Differences in signal intensity made comparison of *Wnt1* expression at E10.5 difficult (Figure A-21), though *Wnt1* expression was weak in the dorsal neural tube of the $Zic2^{+/+}$ embryo and in one of the heterozygotes and strong in the dorsal neural tube of the mutants and one of the heterozygotes.

Similar variability was present in the *in situs* analyzing *Wnt3a* expression. At E9.5, *Wnt3a* was expressed in the dorsal-most neural tube adjacent to the dorsal one-third of the otocyst in mice from all three genotypes (Figure A-22). By E10.5, the *Wnt3a*-expressing region expanded ventrally, encompassing the neural tube adjacent to the dorsal half of the otocyst (Figure A-23). Variation in staining intensity was observed primarily at E10.5. Some of the embryos at E9.5 had otocysts whose shapes more closely resembled that of an E10.5 ear, leading to some "E9.5" embryos having *Wnt3a* expression patterns more similar to that of an E10.5 embryo. Despite these variations, expression of the WNT ligands *Wnt1* and *Wnt3a* appeared to be unchanged in the region of the inner ear in the $Zic2^{Ku/Ku}$ mice.

Additional Otocyst Patterning Genes

Finally, we looked at the expression of *Wnt2b* (dorso-medial otic epithelium/ED; Figure A-24), *Ngn1* (ventro-medial otic epithelium/neuroblasts; Figure A-25), and *Otx2* (ventral otic epithelium/CD; Figure A-26), but conclusions could not be

made due to inconsistent or non-existent staining as well as the lack of replicates (n=1).

Conclusions

Variability in the *in situs*, coupled with low numbers of replicates (n=1 or 2) made it difficult to draw any conclusions from our data about the activation of the SHH, BMP, and WNT signaling pathways, as well as about the status of the expression of pathway components of the FGF, SHH, BMP, and WNT signaling pathways. Further, variability in the extent of the neural tube defects in the *Zic2*$^{Ku/Ku}$ mice, as well as the differing extent of otocyst displacement/rotation resulting from those neural tube defects, adds another layer of complexity to the analysis of the inner ear phenotypes from these mice. Future experiments will need to be carefully controlled so that in addition to having greater numbers of replicates per genotype for each riboprobe, there will also be replicates for each type/degree of severity of neural tube/otocyst defect. This will allow for detection of changes in expression between genotypes as well as any changes in expression resulting from differing degrees of severity of the neural tube closure and otocyst positioning defects.

A.2. Figures

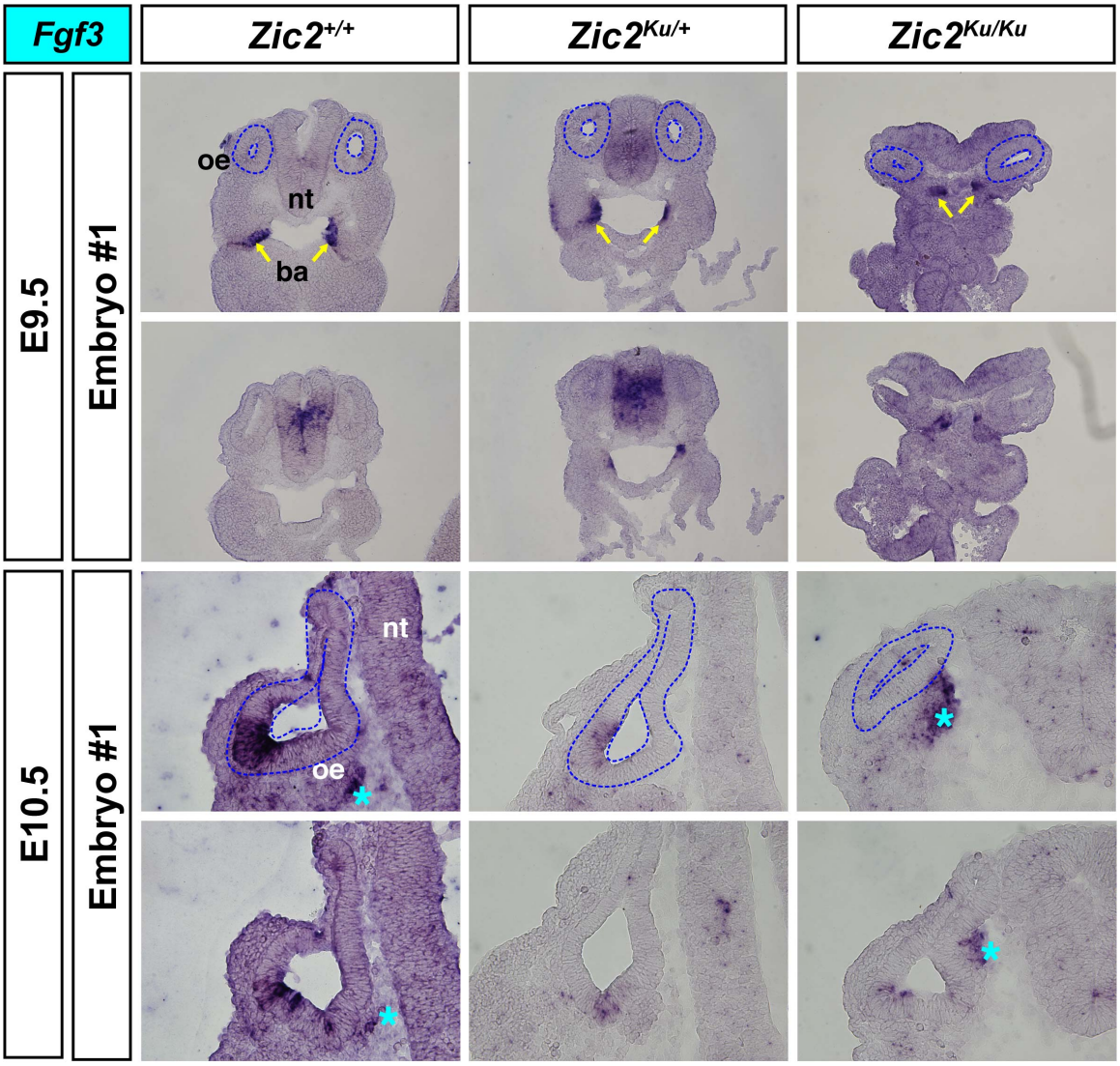

Figure A-1. *Fgf3* expression in the otic region of *Zic2*$^{+/+}$, *Zic2*$^{Ku/+}$, and *Zic2*$^{Ku/Ku}$ mouse embryos at E9.5 and E10.5. *In situ* hybridization on 12µm transverse sections through the otocyst of E9.5 (top 2 rows) and E10.5 (bottom 2 rows) mouse embryos using a probe for *Fgf3*. Abbreviations: oe, otic epithelium; nt, neural tube. Blue dashed line outlines the otic epithelium. Light blue asterisks highlight mesenchymal expression. Top and bottom sections within each embryo cluster ("embryo #1") are from different levels of the ear in the same embryo. **[n=1 for all genotypes at both E9.5 and E10.5]**

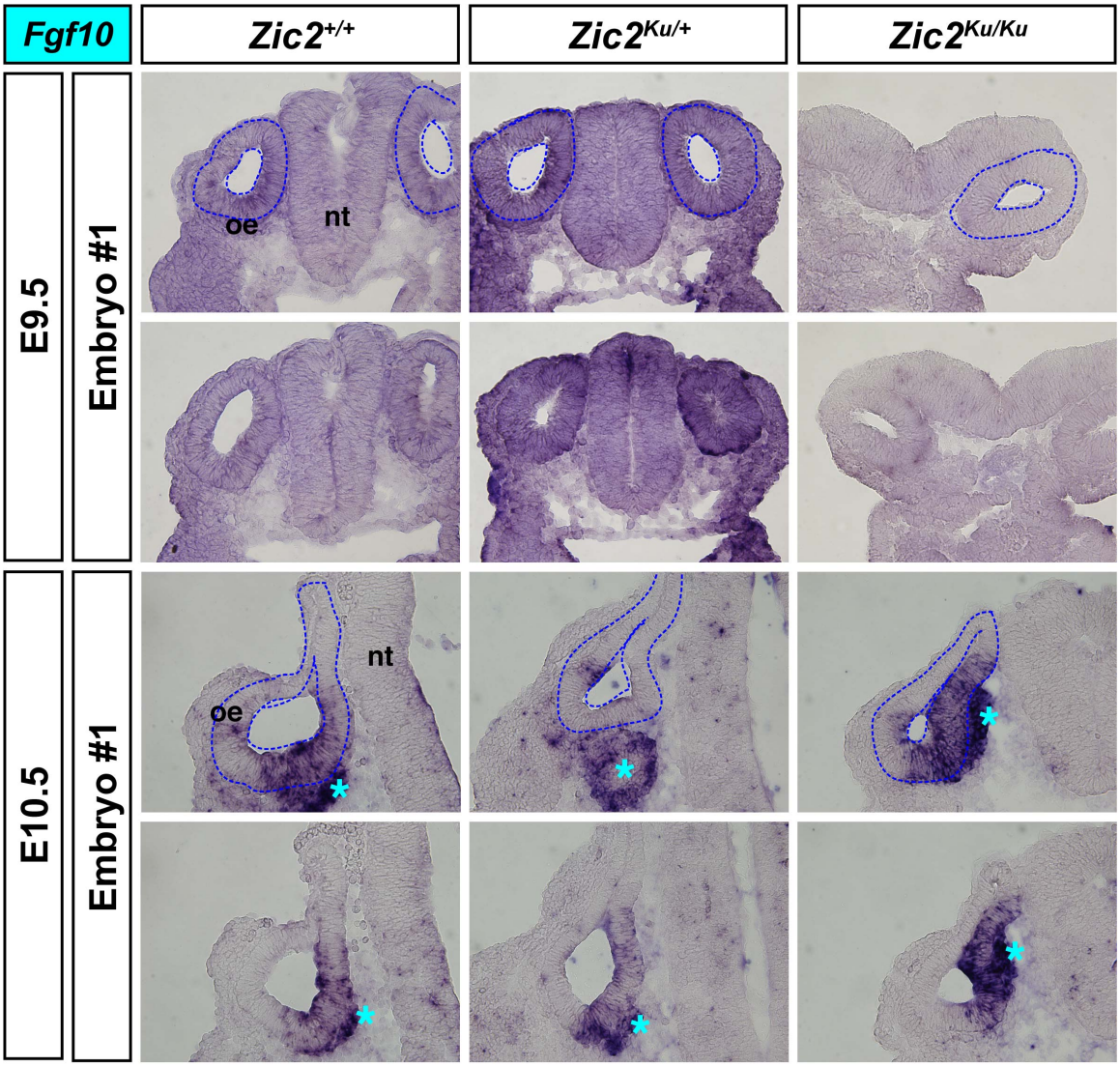

Figure A-2. *Fgf10* expression in the otic region of *Zic2*$^{+/+}$, *Zic2*$^{Ku/+}$, and *Zic2*$^{Ku/Ku}$ mouse embryos at E9.5 and E10.5. *In situ* hybridization on 12µm transverse sections through the otocyst of E9.5 (top 2 rows) and E10.5 (bottom 2 rows) mouse embryos using a probe for *Fgf10*. Abbreviations: oe, otic epithelium; nt, neural tube. Blue dashed line outlines the otic epithelium. Light blue asterisks highlight mesenchymal expression. Top and bottom sections within each embryo cluster ("embryo #1") are from different levels of the ear in the same embryo. **[n=1 for all genotypes at both E9.5 and E10.5]**

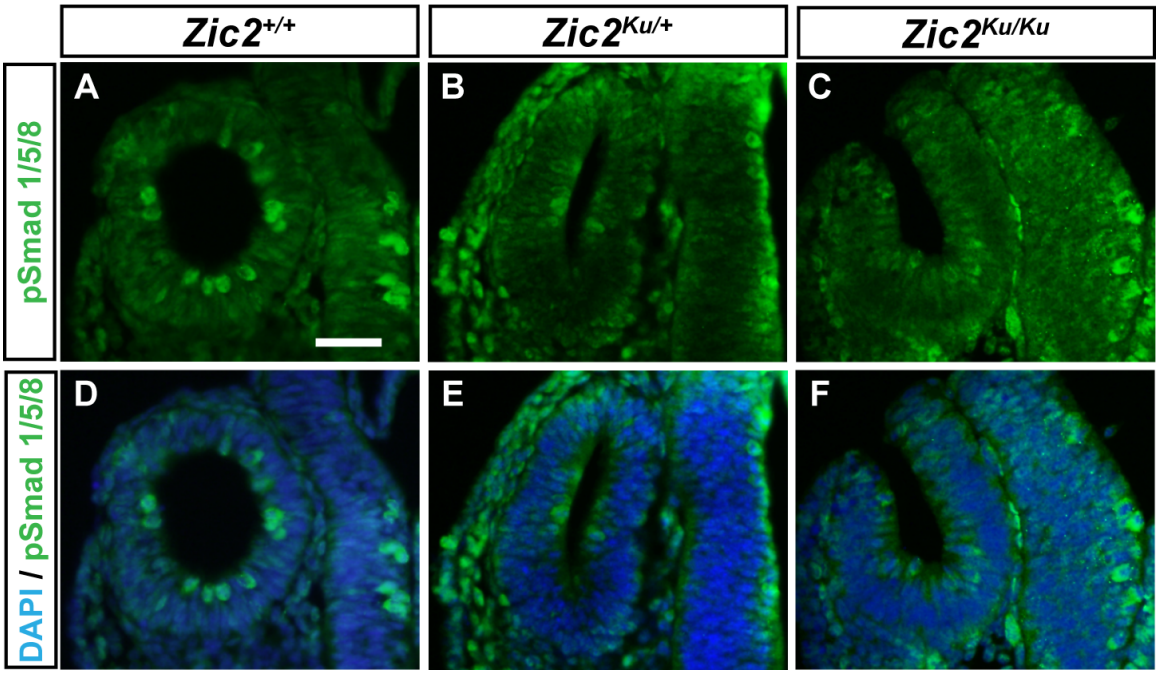

Figure A-3. Comparison of BMP Pathway Activation in the Developing Inner Ear at E9.5 in the *Zic2*^{Ku} Mouse Model. Immunofluorescence experiments using phospho-Smad-1/5/8 antibody were performed on sections through the inner ear region from *Zic2*$^{+/+}$ (A, D), *Zic2*$^{Ku/+}$ (B, E), and *Zic2*$^{Ku/Ku}$ (C, F) mice. (A-C) Phospho-Smad-1/5/8 (green), (D-F) Phospho-Smad-1/5/8 (green) and nuclei (blue). Scale bar in A, 50μm (applies to A-F). **[n=2 for *Zic2*$^{+/+}$ and *Zic2*$^{Ku/+}$; n=1 for *Zic2*$^{Ku/Ku}$]**

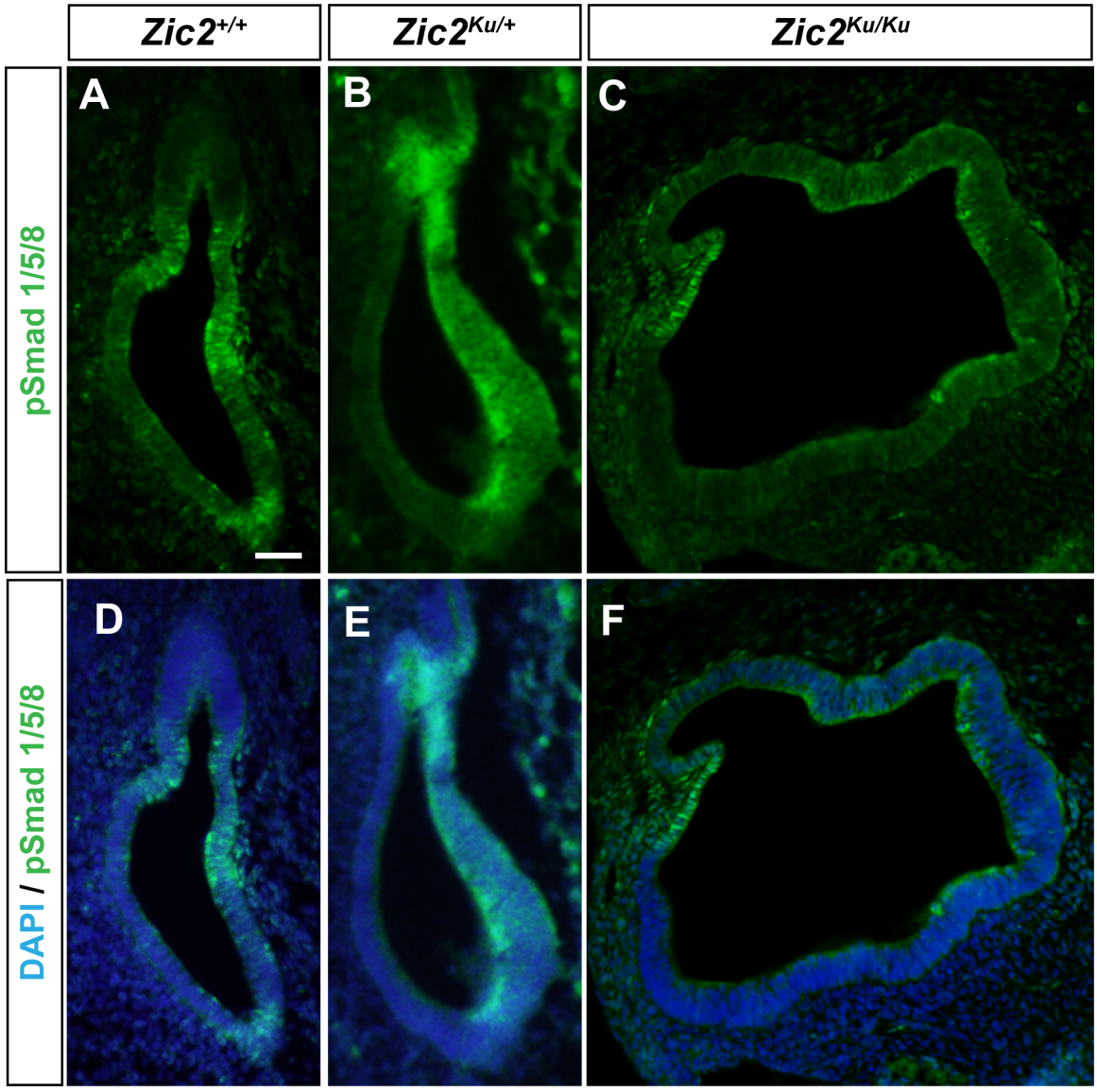

Figure A-4. Comparison of BMP Pathway Activation in the Developing Inner Ear at E11.5 in the *Zic2*^{Ku} Mouse Model. Immunofluorescence experiments using phospho-Smad-1/5/8 antibody were performed on sections through the inner ear region from *Zic2*$^{+/+}$ (A, D), *Zic2*$^{Ku/+}$ (B, E), and *Zic2*$^{Ku/Ku}$ (C, F) mice. (A-C) Phospho-Smad-1/5/8 (green), (D-F) Phospho-Smad-1/5/8 (green) and nuclei (blue). Scale bar in A, 200μm (applies to A-F). **[n=2 for all genotypes]**

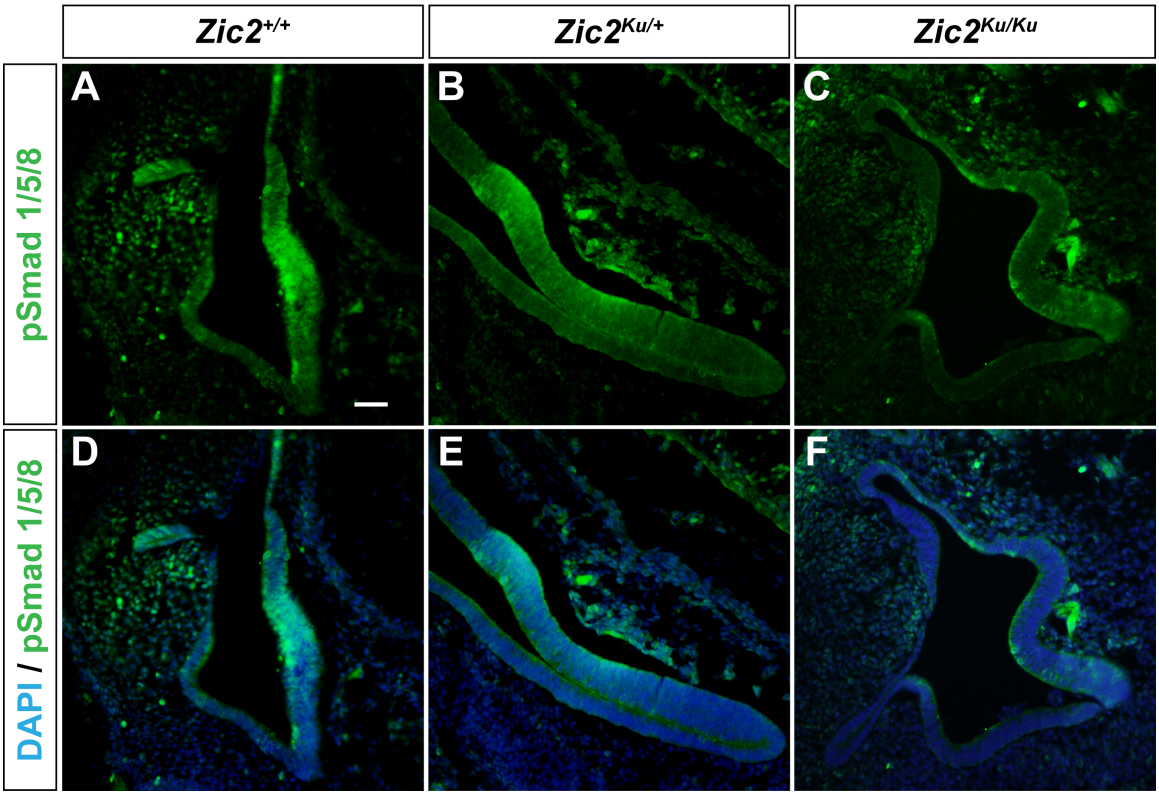

Figure A-5. Comparison of BMP Pathway Activation in the Developing Inner Ear at E12.5 in the *Zic2*^{Ku} Mouse Model. Immunofluorescence experiments using phospho-Smad-1/5/8 antibody were performed on sections through the inner ear region from *Zic2*$^{+/+}$ (A, D), *Zic2*$^{Ku/+}$ (B, E), and *Zic2*$^{Ku/Ku}$ (C, F) mice. (A-C) Phospho-Smad-1/5/8 (green), (D-F) Phospho-Smad-1/5/8 (green) and nuclei (blue). Scale bar in A, 200μm (applies to A-F). **[n=2 for all genotypes]**

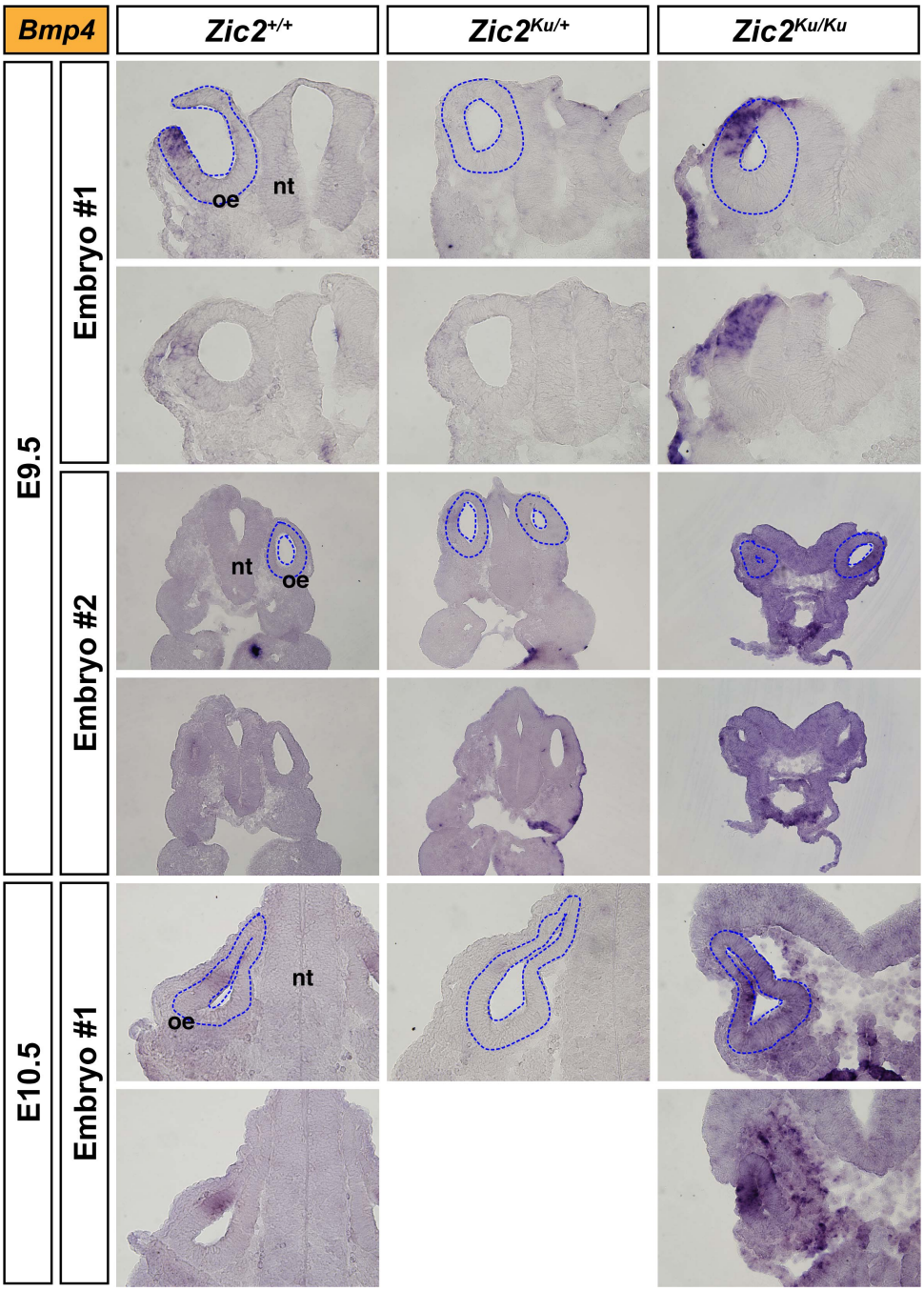

Figure A-6. *Bmp4* expression in the otic region of *Zic2*$^{+/+}$, *Zic2*$^{Ku/+}$, and *Zic2*$^{Ku/Ku}$ mouse embryos at E9.5 and E10.5. *In situ* hybridization on 12µm transverse sections through the otocyst of E9.5 (top 4 rows) and E10.5 (bottom 2 rows) mouse embryos using a probe for *Bmp4*. Abbreviations: oe, otic epithelium; nt, neural tube. Blue dashed line outlines the otic epithelium. Top and bottom sections within each embryo cluster ("embryo #1", "embryo #2") are from different levels of the ear in the same embryo. **[E9.5: n=2 for all genotypes; E10.5: n=1 for all genotypes]**

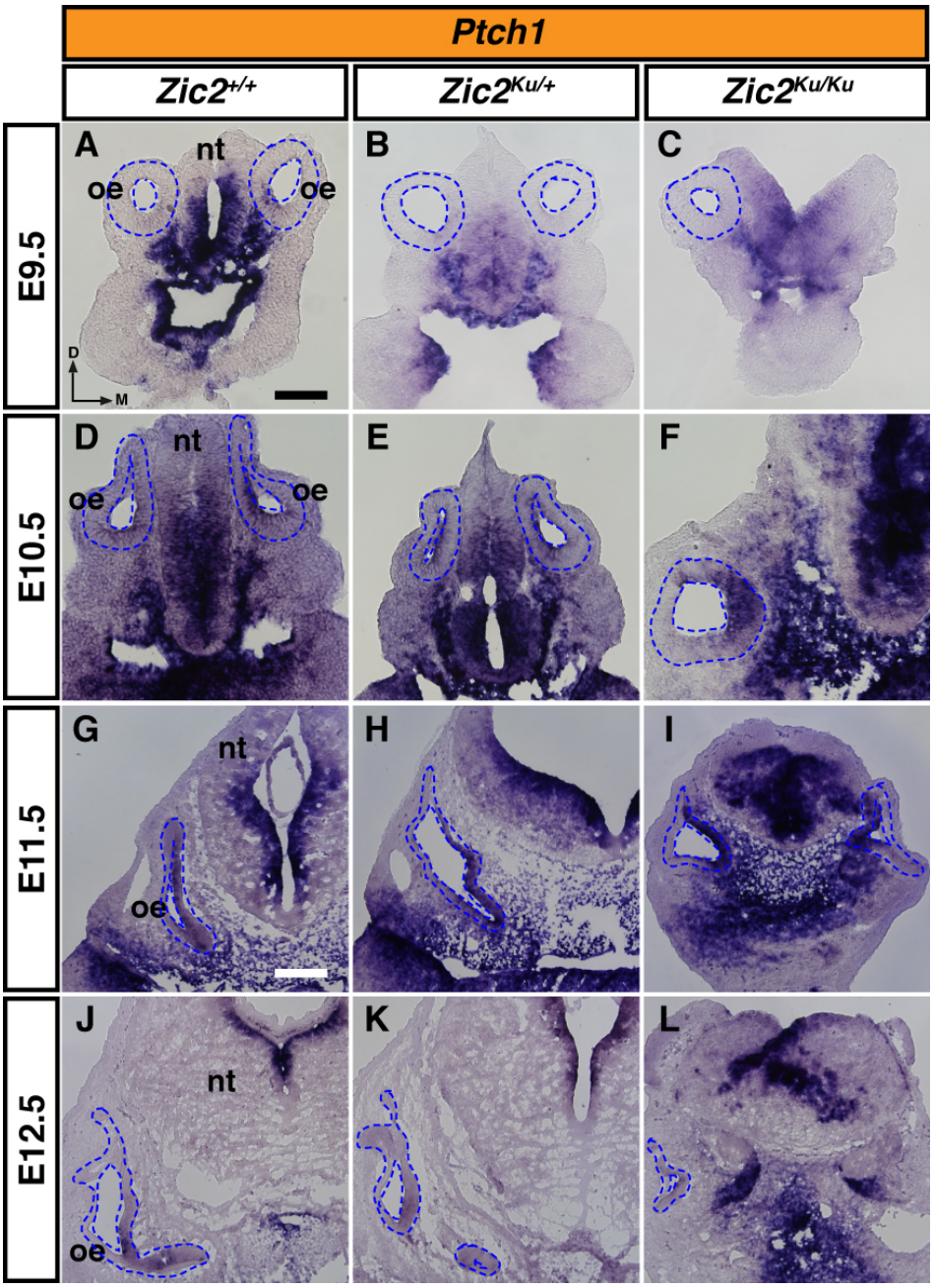

Figure A-7. Comparison of SHH Pathway Activation in the Developing Inner Ear in the *Zic2*^{Ku} Mouse Model. *In situ* hybridization using a probe for *Ptch1* was performed on sections through the inner ear region of *Zic2*$^{+/+}$ (A, D, G, J), *Zic2*$^{Ku/+}$ (B, E, H, K), and *Zic2*$^{Ku/Ku}$ (C, F, I, L) embryos at E9.5 (A-C), E10.5 (D-F), E11.5 (G-I), and E12.5 (J-L). Blue dashed lines outline the otic epithelium. Abbreviations: oe, otic epithelium; nt, neural tube; d, dorsal; m, medial. Scale bar in A, 50μm (applies to A-F); scale bar in G, 200μm (applies to G-L). **[E9.5: n=2 for *Zic2*$^{+/+}$, n=3 for *Zic2*$^{Ku/+}$ and *Zic2*$^{Ku/Ku}$; E10.5: n=1 for *Zic2*$^{+/+}$; n=2 for *Zic2*$^{Ku/+}$ and *Zic2*$^{Ku/Ku}$; E11.5: n=3 for *Zic2*$^{+/+}$ and *Zic2*$^{Ku/Ku}$; n=2 for *Zic2*$^{Ku/+}$; E12.5: n=3 for *Zic2*$^{+/+}$ and *Zic2*$^{Ku/Ku}$; n=2 for *Zic2*$^{Ku/+}$]**

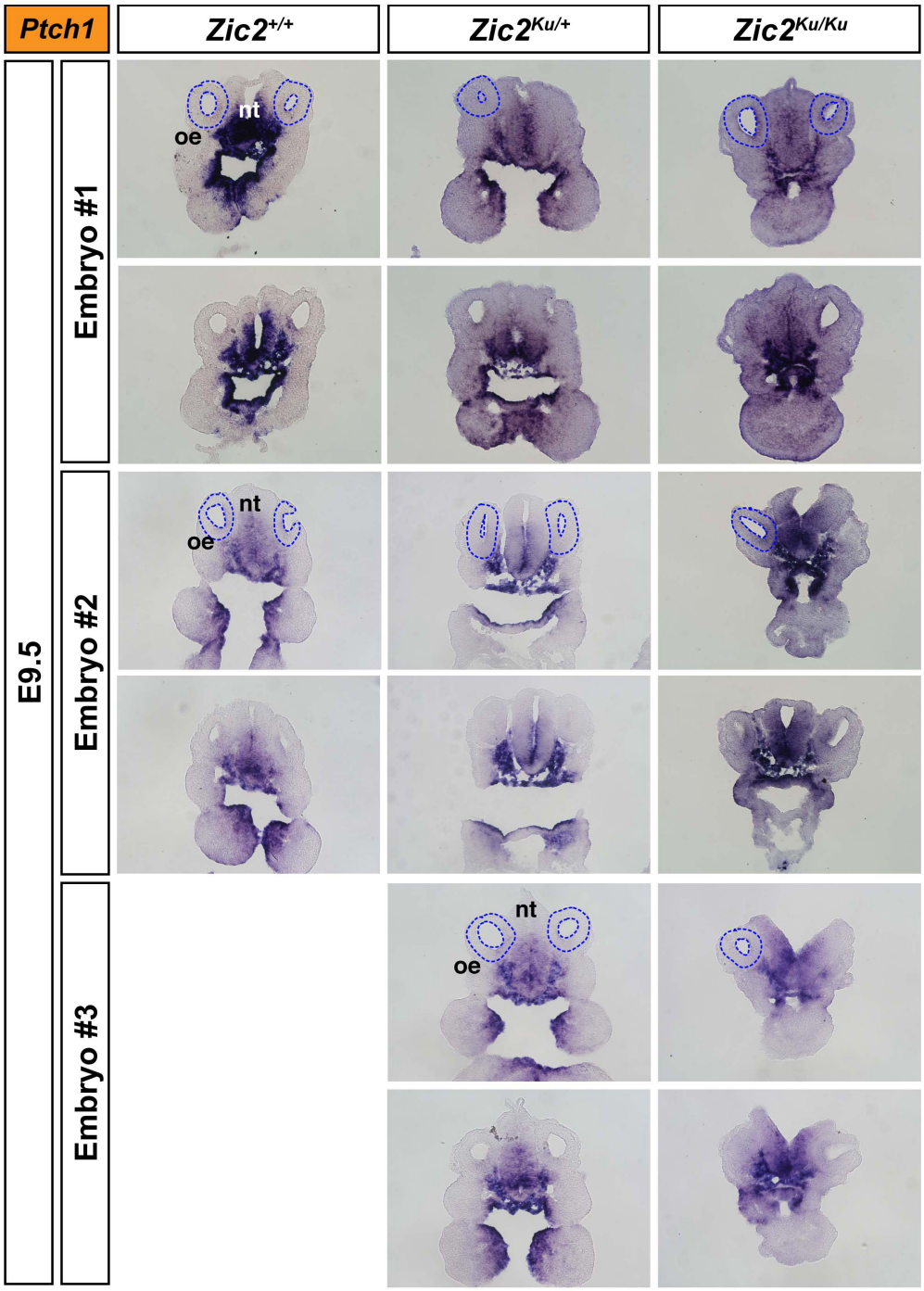

Figure A-8. *Ptch1* expression in the otic region of *Zic2*$^{+/+}$, *Zic2*$^{Ku/+}$, and *Zic2*$^{Ku/Ku}$ mouse embryos at E9.5. *In situ* hybridization on 12µm transverse sections through the otocyst of E9.5 mouse embryos using a probe for *Ptch1*. Abbreviations: oe, otic epithelium; nt, neural tube. Blue dashed line outlines the otic epithelium. Top and bottom sections within each embryo cluster ("embryo #1", "embryo #2", "embryo #3") are from different levels of the ear in the same embryo. **[n=2 for *Zic2*$^{+/+}$; n=3 for *Zic2*$^{Ku/+}$ and *Zic2*$^{Ku/Ku}$]**

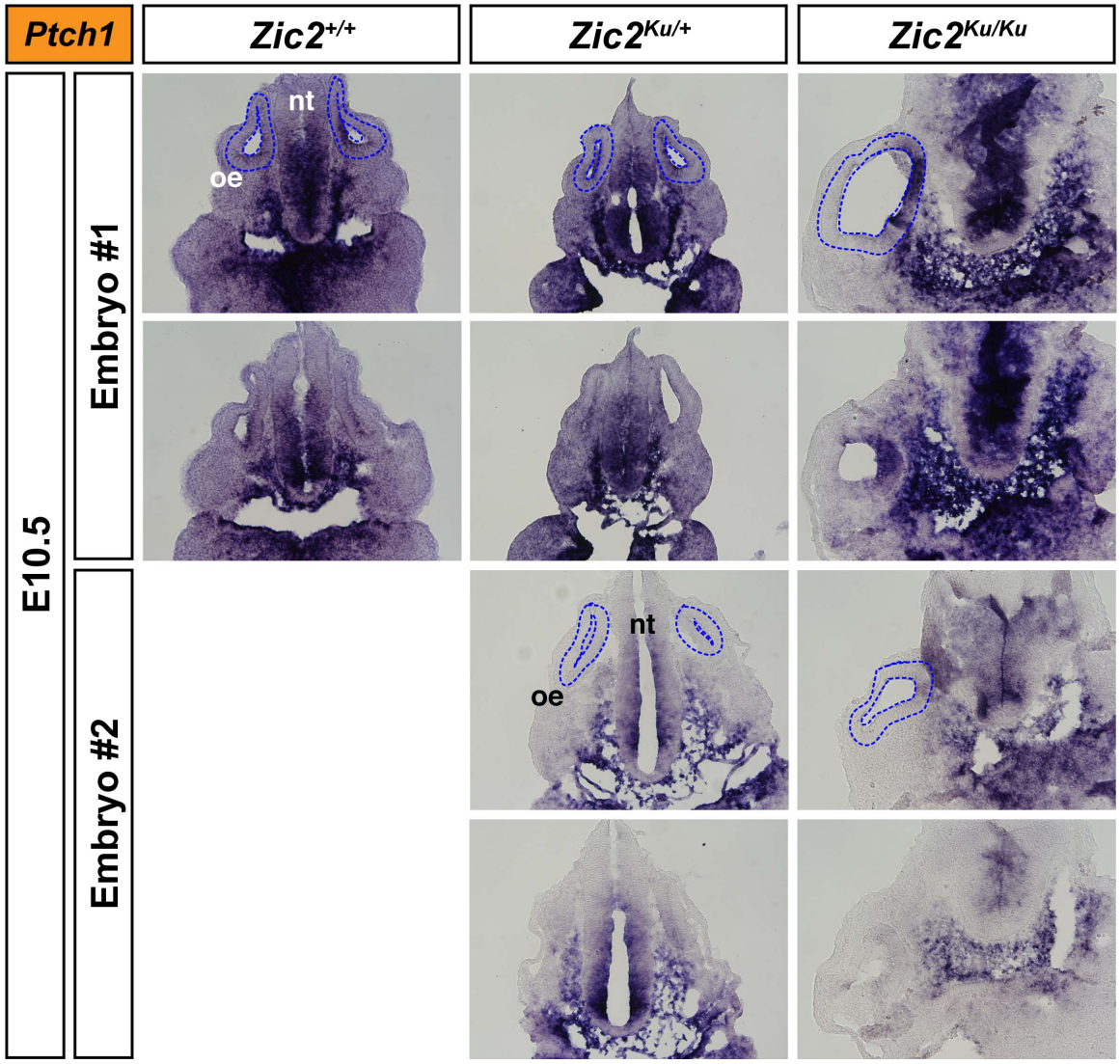

Figure A-9. *Ptch1* expression in the otic region of *Zic2*$^{+/+}$, *Zic2*$^{Ku/+}$, and *Zic2*$^{Ku/Ku}$ mouse embryos at E10.5. *In situ* hybridization on 12µm transverse sections through the otocyst of E10.5 mouse embryos using a probe for *Ptch1*. Abbreviations: oe, otic epithelium; nt, neural tube. Blue dashed line outlines the otic epithelium. Top and bottom sections within each embryo cluster ("embryo #1", "embryo #2") are from different levels of the ear in the same embryo. **[n=1 for *Zic2*$^{+/+}$; n=2 for *Zic2*$^{Ku/+}$ and *Zic2*$^{Ku/Ku}$]**

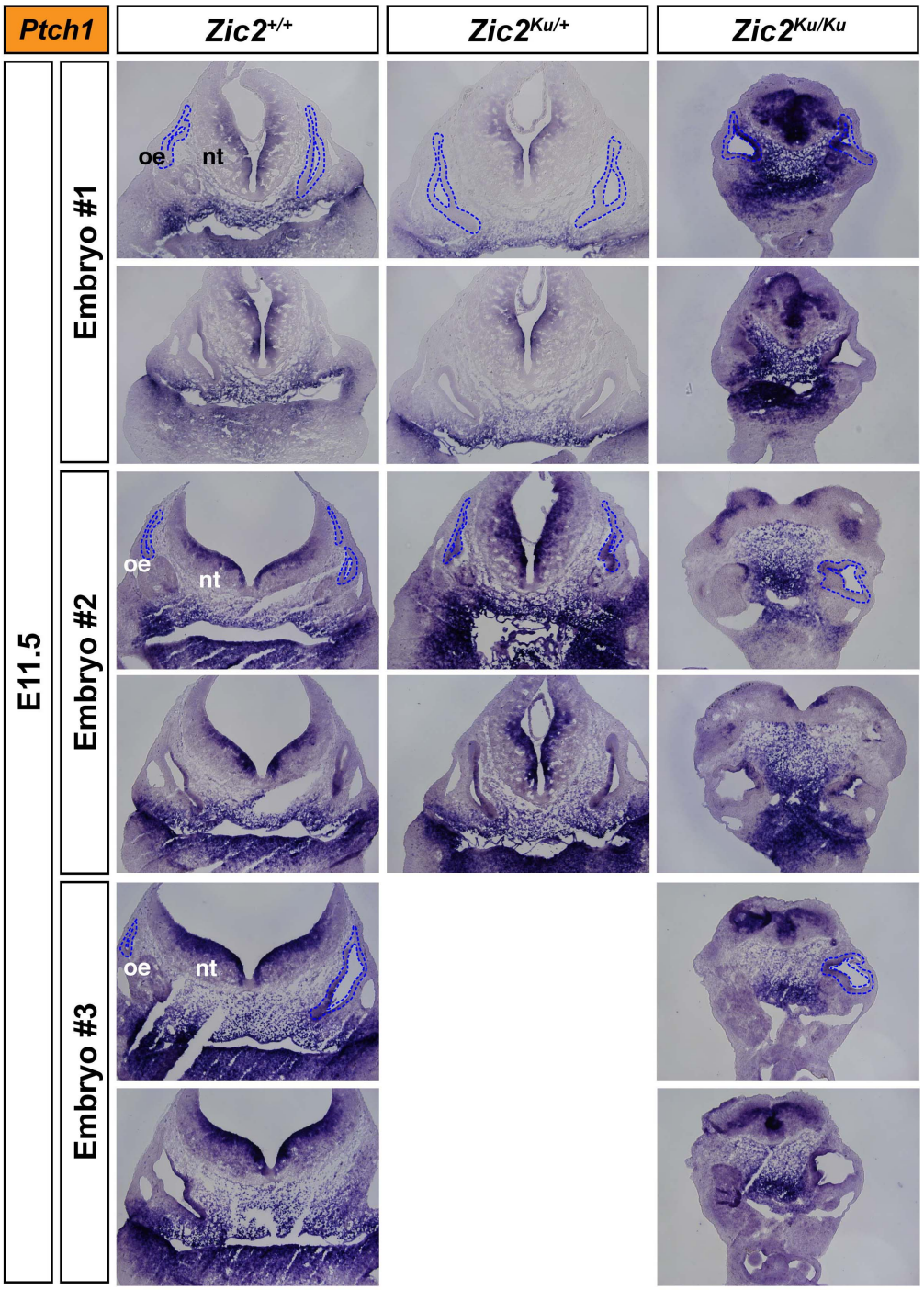

Figure A-10. *Ptch1* expression in the otic region of *Zic2*$^{+/+}$, *Zic2*$^{Ku/+}$, and *Zic2*$^{Ku/Ku}$ mouse embryos at E11.5. *In situ* hybridization on 12µm transverse sections through the otocyst of E11.5 mouse embryos using a probe for *Ptch1*. Abbreviations: oe, otic epithelium; nt, neural tube. Blue dashed line outlines the otic epithelium. Top and bottom sections within each embryo cluster ("embryo #1", "embryo #2", "embryo #3") are from different levels of the ear in the same embryo. **[n=3 for *Zic2*$^{+/+}$ and *Zic2*$^{Ku/Ku}$; n=2 for *Zic2*$^{Ku/+}$]**

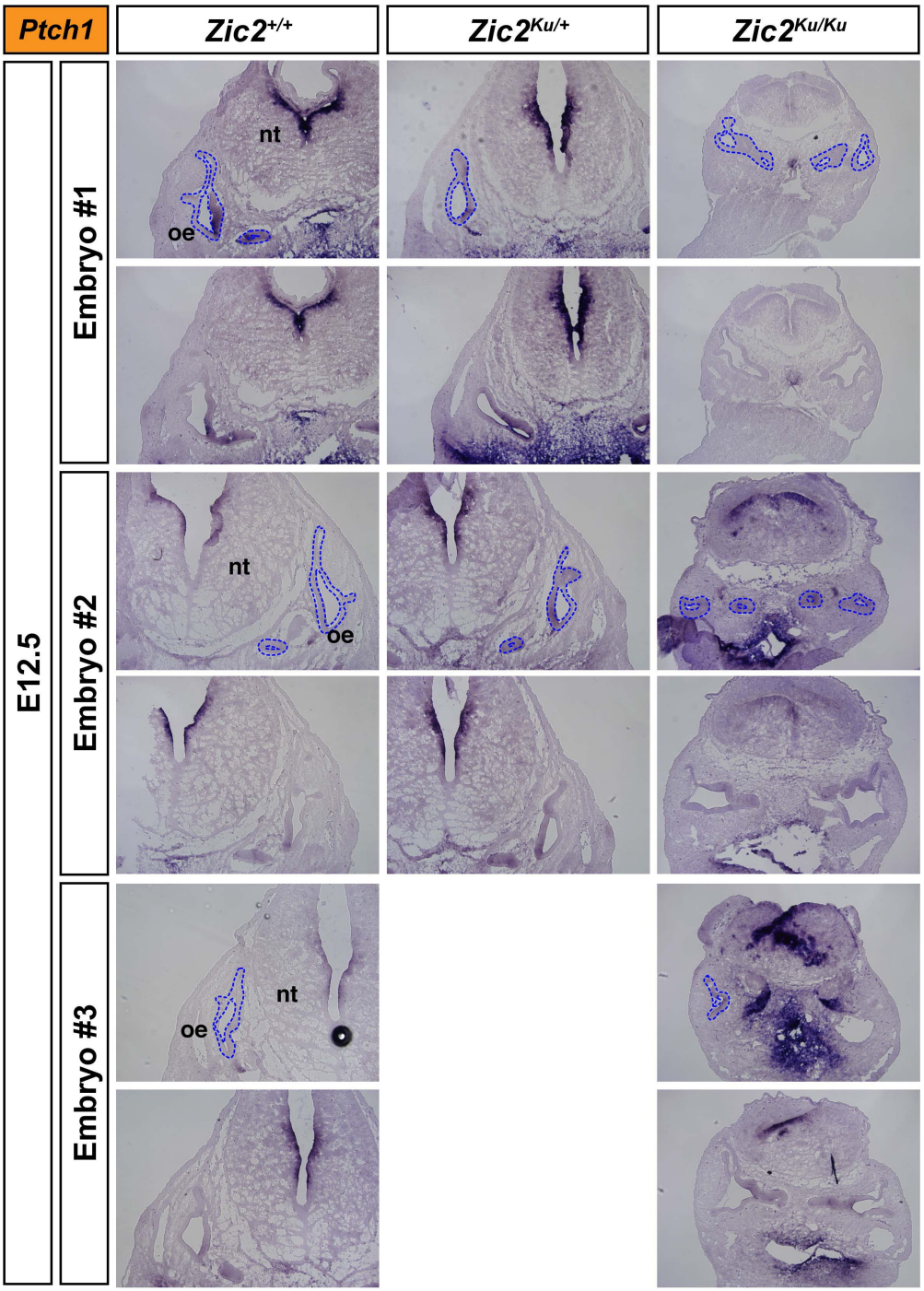

Figure A-11. *Ptch1* expression in the otic region of *Zic2*$^{+/+}$, *Zic2*$^{Ku/+}$, and *Zic2*$^{Ku/Ku}$ mouse embryos at E12.5. *In situ* hybridization on 12µm transverse sections through the otocyst of E12.5 mouse embryos using a probe for *Ptch1*. Abbreviations: oe, otic epithelium; nt, neural tube. Blue dashed line outlines the otic epithelium. Top and bottom sections within each embryo cluster ("embryo #1", "embryo #2", "embryo #3") are from different levels of the ear in the same embryo. **[n=3 for *Zic2*$^{+/+}$ and *Zic2*$^{Ku/Ku}$; n=2 for *Zic2*$^{Ku/+}$]**

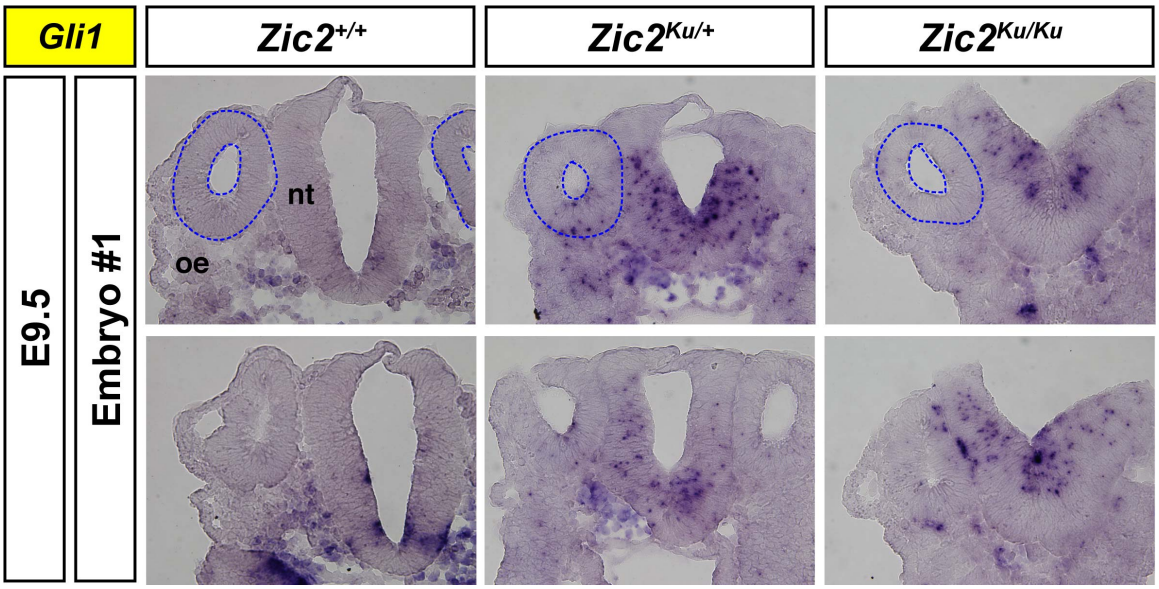

Figure A-12. *Gli1* expression in the otic region of *Zic2*$^{+/+}$, *Zic2*$^{Ku/+}$, and *Zic2*$^{Ku/Ku}$ mouse embryos at E9.5. *In situ* hybridization on 12µm transverse sections through the otocyst of E9.5 mouse embryos using a probe for *Gli1*. Abbreviations: oe, otic epithelium; nt, neural tube. Blue dashed line outlines the otic epithelium. Top and bottom sections within each embryo cluster ("embryo #1") are from different levels of the ear in the same embryo. **[n=1 for all genotypes]**

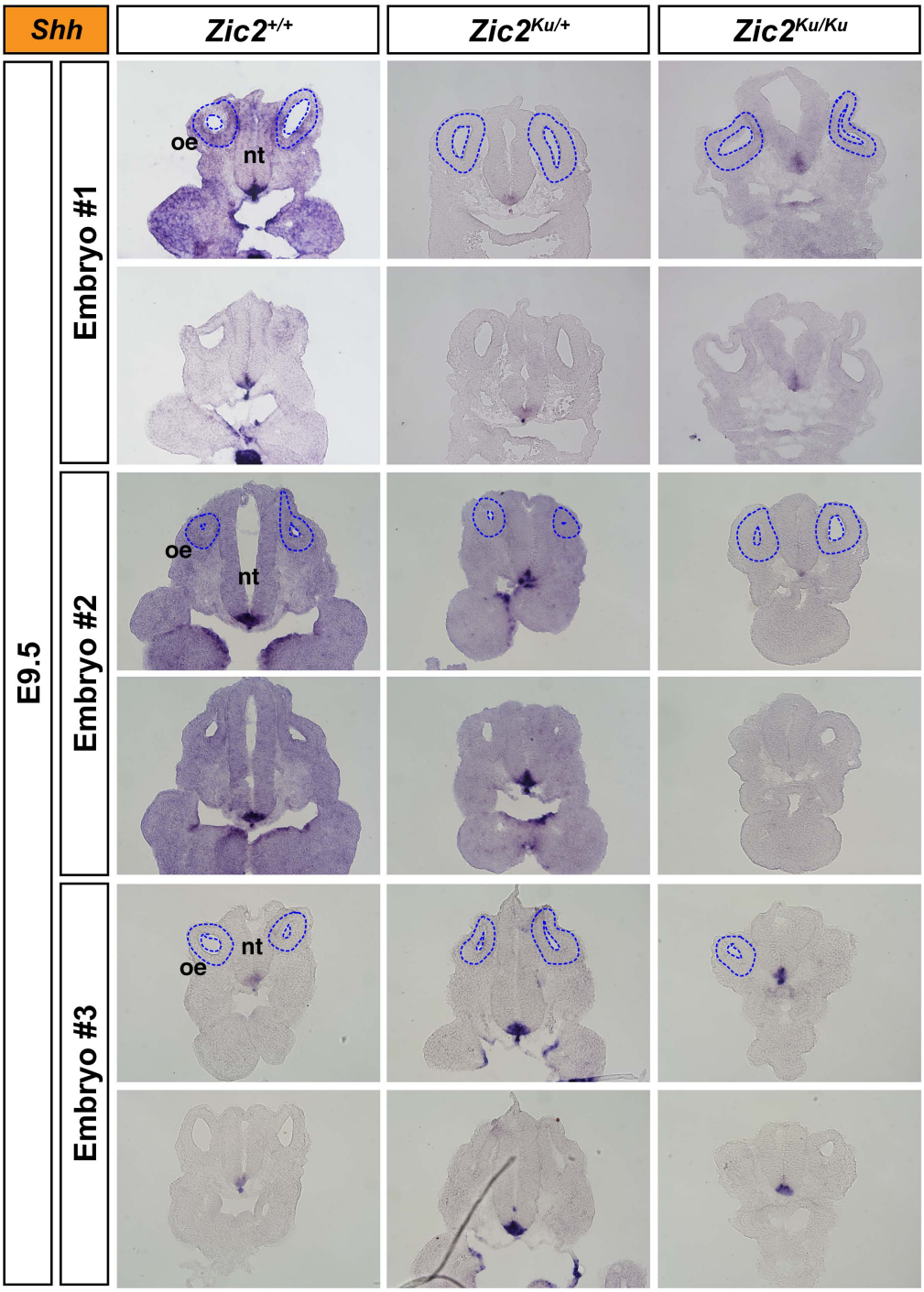

Figure A-13. *Shh* expression in the otic region of *Zic2*$^{+/+}$, *Zic2*$^{Ku/+}$, and *Zic2*$^{Ku/Ku}$ mouse embryos at E9.5. *In situ* hybridization on 12µm transverse sections through the otocyst of E9.5 mouse embryos using a probe for *Shh*. Abbreviations: oe, otic epithelium; nt, neural tube. Blue dashed line outlines the otic epithelium. Top and bottom sections within each embryo cluster ("embryo #1", "embryo #2", "embryo #3") are from different levels of the ear in the same embryo. **[n=3 for all genotypes]**

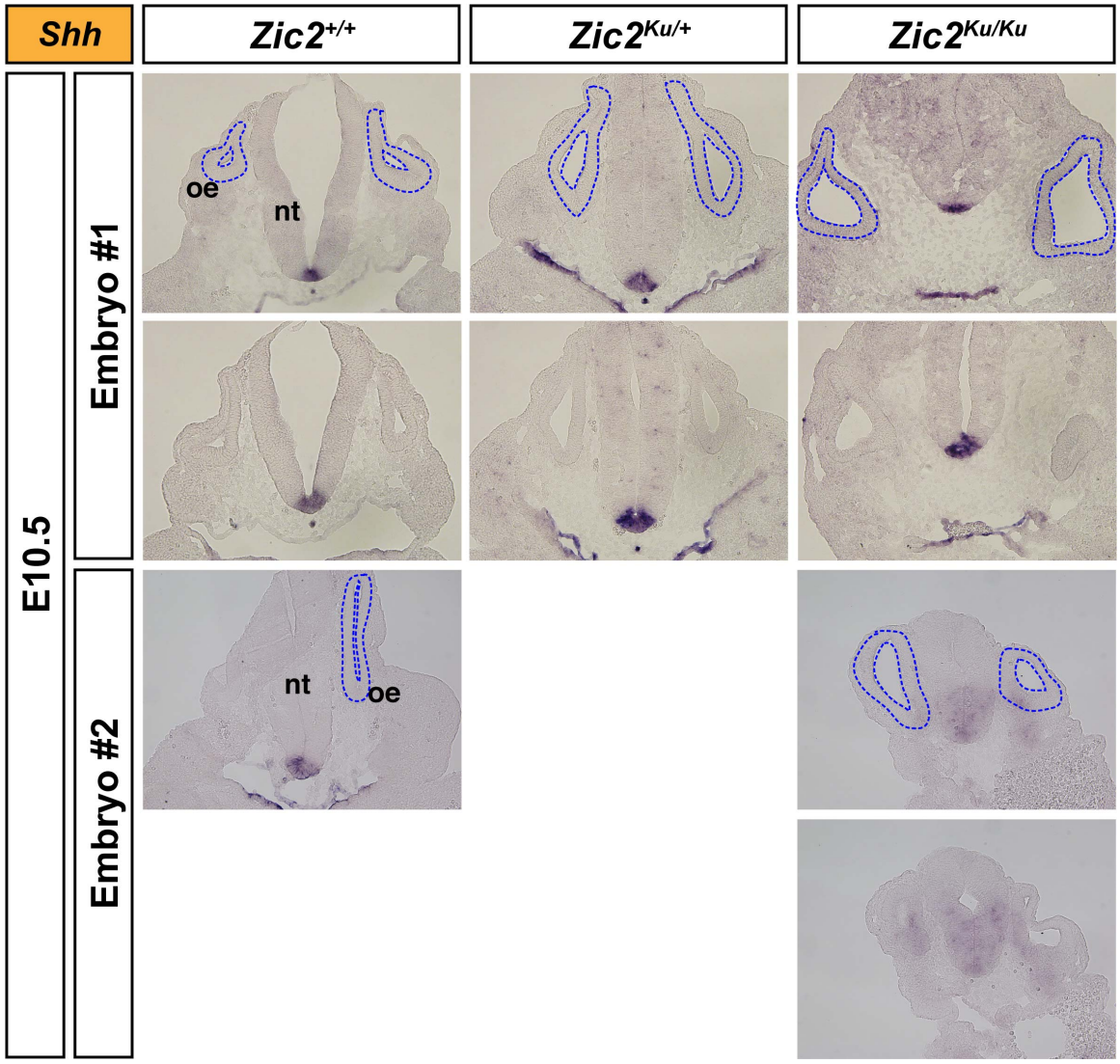

Figure A-14. *Shh* expression in the otic region of *Zic2*$^{+/+}$, *Zic2*$^{Ku/+}$, and *Zic2*$^{Ku/Ku}$ mouse embryos at E10.5. *In situ* hybridization on 12µm transverse sections through the otocyst of E10.5 mouse embryos using a probe for *Shh*. Abbreviations: oe, otic epithelium; nt, neural tube. Blue dashed line outlines the otic epithelium. Top and bottom sections within each embryo cluster ("embryo #1", "embryo #2") are from different levels of the ear in the same embryo. **[n=2 for *Zic2*$^{+/+}$ and *Zic2*$^{Ku/Ku}$; n=1 for *Zic2*$^{Ku/+}$]**

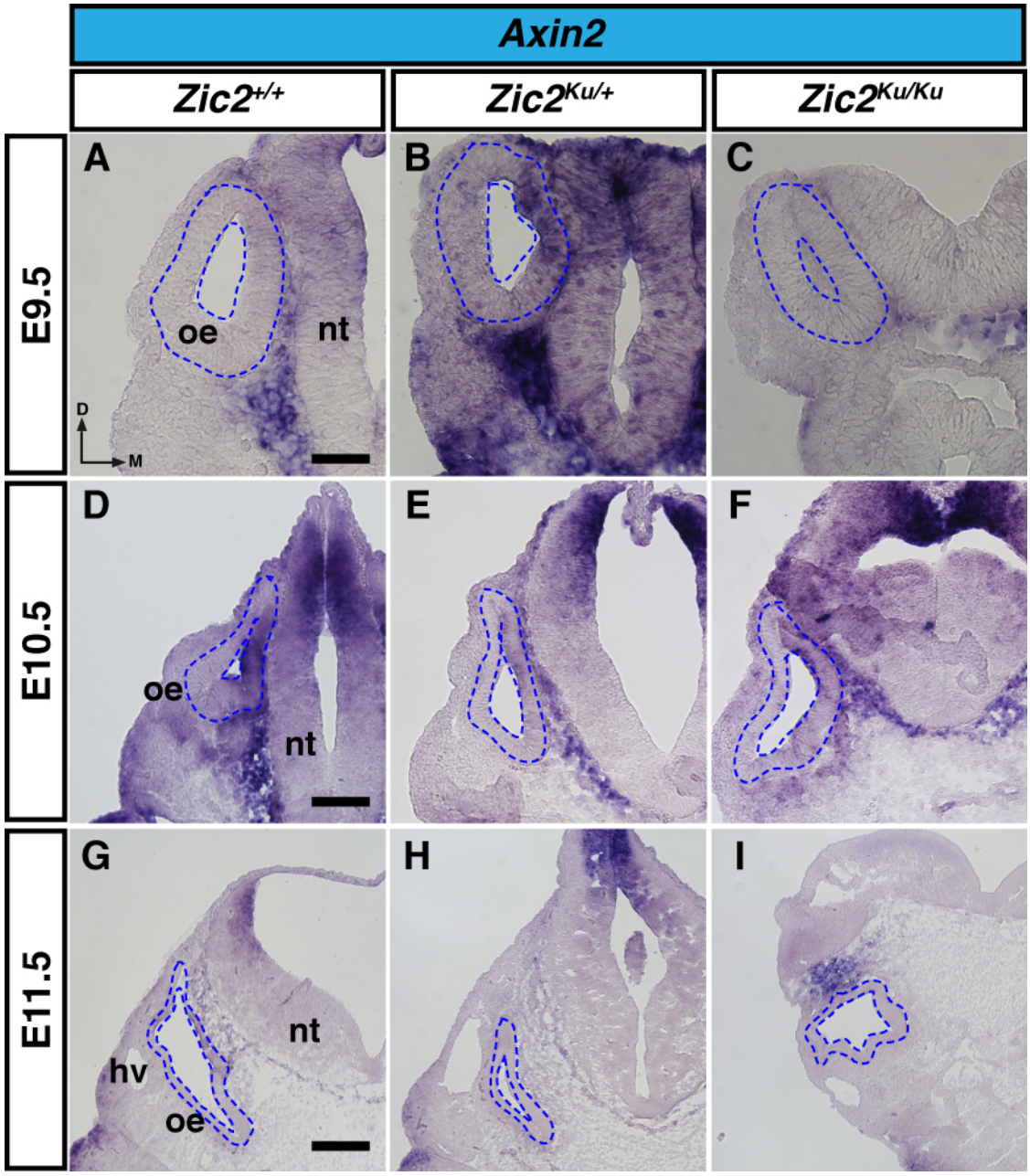

Figure A-15. Comparison of WNT Pathway Activation in the Developing Inner Ear in the *Zic2*^{Ku} Mouse Model. *In situ* hybridization using a probe for *Axin2* was performed on sections through the inner ear region of *Zic2*$^{+/+}$ (A, D, G), *Zic2*$^{Ku/+}$ (B, E, H), and *Zic2*$^{Ku/Ku}$ (C, F, I) embryos at E9.5 (A-C), E10.5 (D-F), and E11.5 (G-I). Blue dashed lines outline the otic epithelium. Abbreviations: oe, otic epithelium; nt, neural tube; d, dorsal; m, medial. Scale bar in A, 50μm (applies to A-C); scale bar in D, 100μm (applies to D-F); scale bar in G, 200μm (applies to G-I). **[E9.5: n=3 for all genotypes; E10.5: n=1 for *Zic2*$^{+/+}$, n=2 for *Zic2*$^{Ku/+}$ and *Zic2*$^{Ku/Ku}$; E11.5: n=2 for *Zic2*$^{+/+}$ and *Zic2*$^{Ku/+}$, n=3 for *Zic2*$^{Ku/Ku}$]**

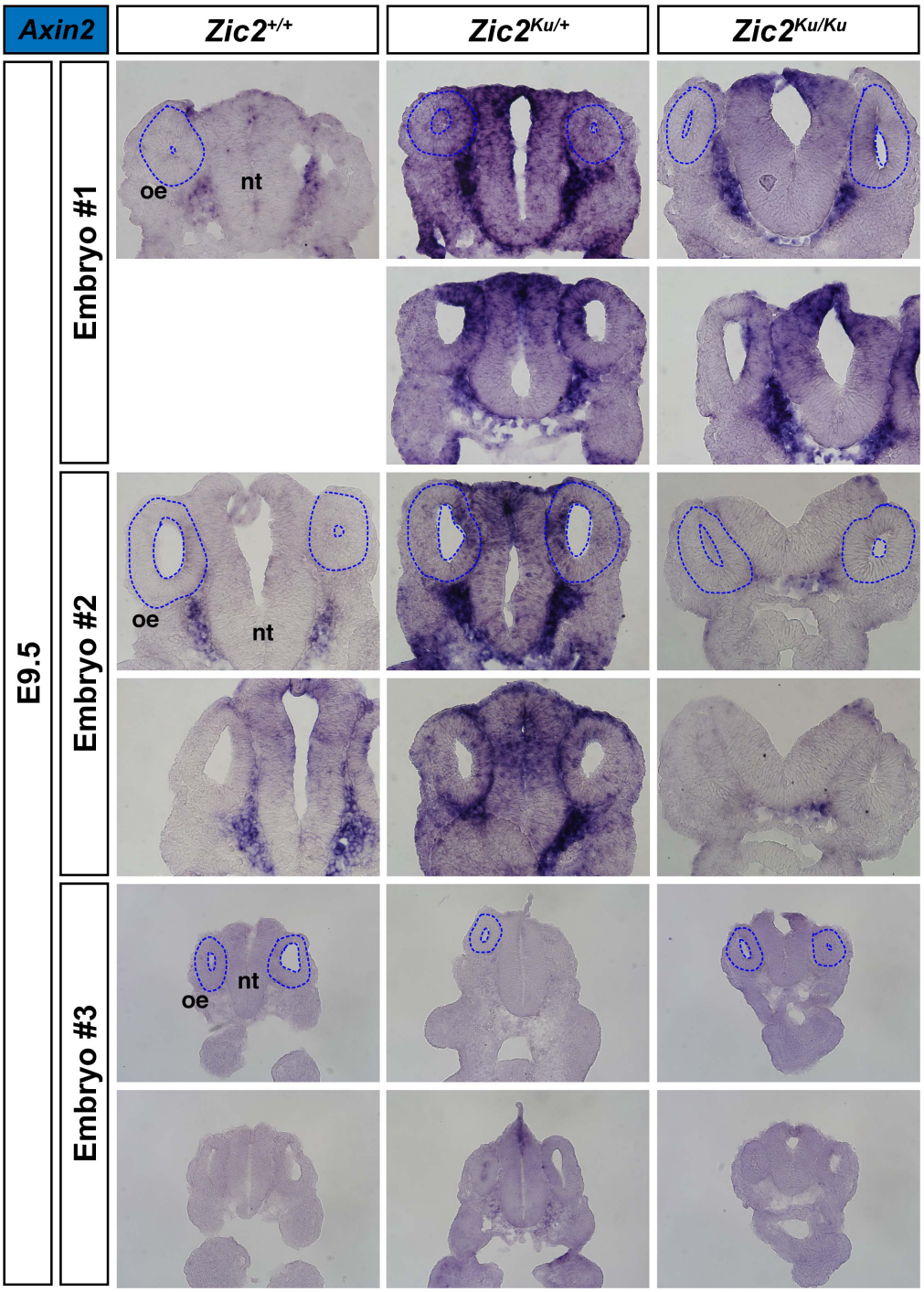

Figure A-16. *Axin2* expression in the otic region of *Zic2*$^{+/+}$, *Zic2*$^{Ku/+}$, and *Zic2*$^{Ku/Ku}$ mouse embryos at E9.5. *In situ* hybridization on 12µm transverse sections through the otocyst of E9.5 mouse embryos using a probe for *Axin2*. Abbreviations: oe, otic epithelium; nt, neural tube. Blue dashed line outlines the otic epithelium. Top and bottom sections within each embryo cluster ("embryo #1", "embryo #2", "embryo #3") are from different levels of the ear in the same embryo. **[n=3 for all genotypes]**

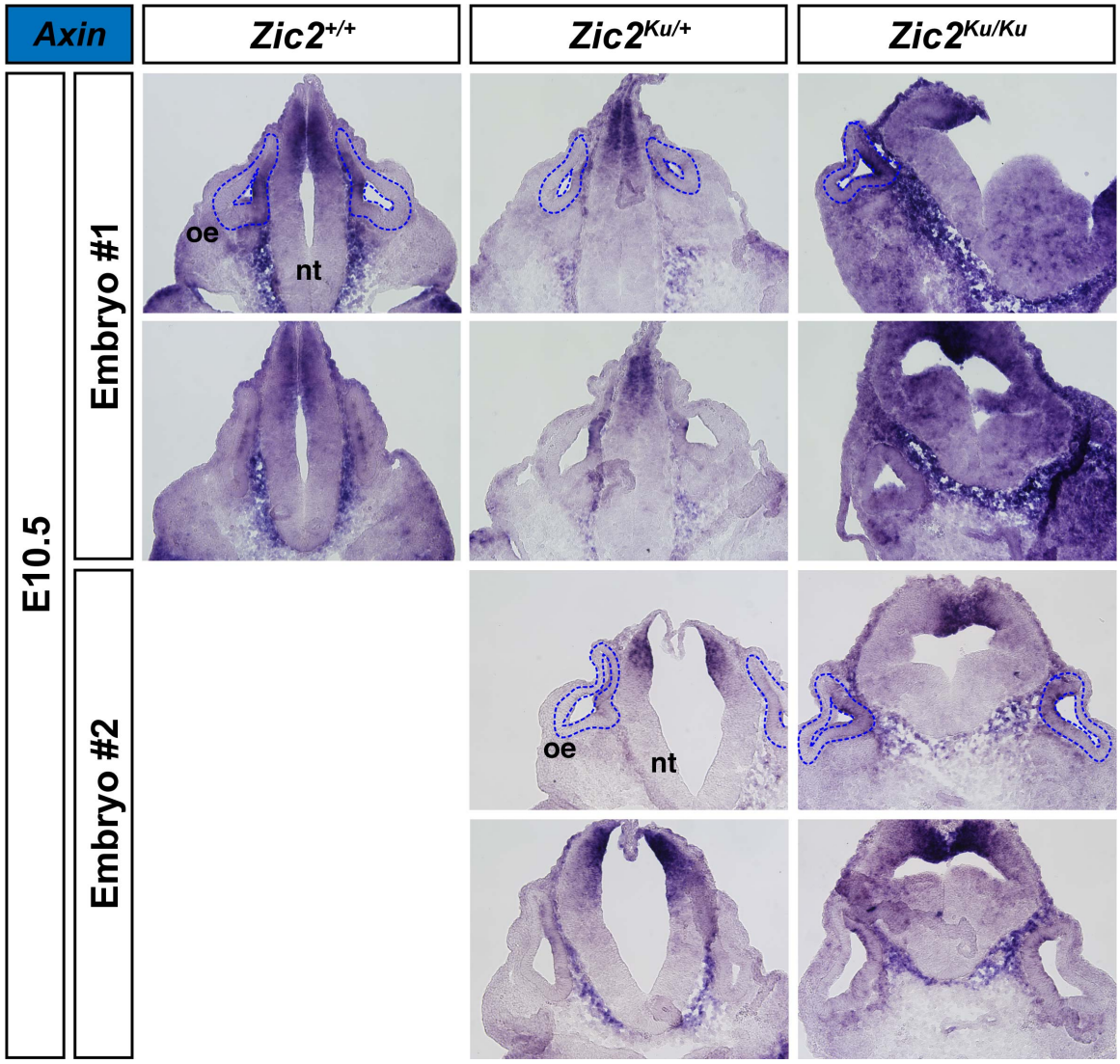

Figure A-17. *Axin2* expression in the otic region of *Zic2*$^{+/+}$, *Zic2*$^{Ku/+}$, and *Zic2*$^{Ku/Ku}$ mouse embryos at E10.5. *In situ* hybridization on 12μm transverse sections through the otocyst of E10.5 mouse embryos using a probe for *Axin2*. Abbreviations: oe, otic epithelium; nt, neural tube. Blue dashed line outlines the otic epithelium. Top and bottom sections within each embryo cluster ("embryo #1", "embryo #2") are from different levels of the ear in the same embryo. **[n=1 for *Zic2*$^{+/+}$; n=2 for *Zic2*$^{Ku/+}$ and *Zic2*$^{Ku/Ku}$]**

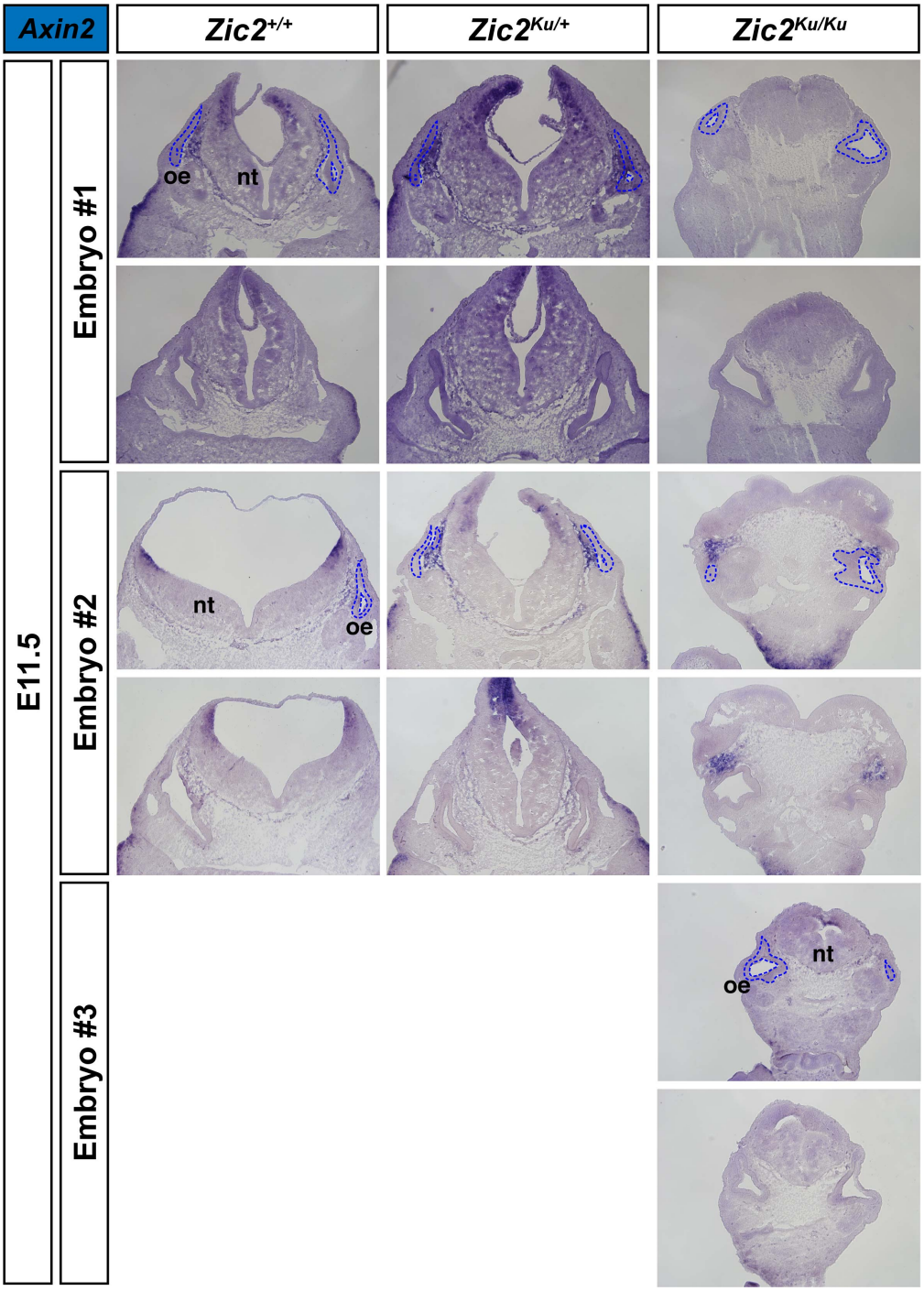

Figure A-18. *Axin2* expression in the otic region of *Zic2*$^{+/+}$, *Zic2*$^{Ku/+}$, and *Zic2*$^{Ku/Ku}$ mouse embryos at E11.5. *In situ* hybridization on 12µm transverse sections through the otocyst of E11.5 mouse embryos using a probe for *Axin2*. Abbreviations: oe, otic epithelium; nt, neural tube. Blue dashed line outlines the otic epithelium. Top and bottom sections within each embryo cluster ("embryo #1", "embryo #2", "embryo #3") are from different levels of the ear in the same embryo. **[n=2 for *Zic2*$^{+/+}$ and *Zic2*$^{Ku/+}$; n=3 for *Zic2*$^{Ku/Ku}$]**

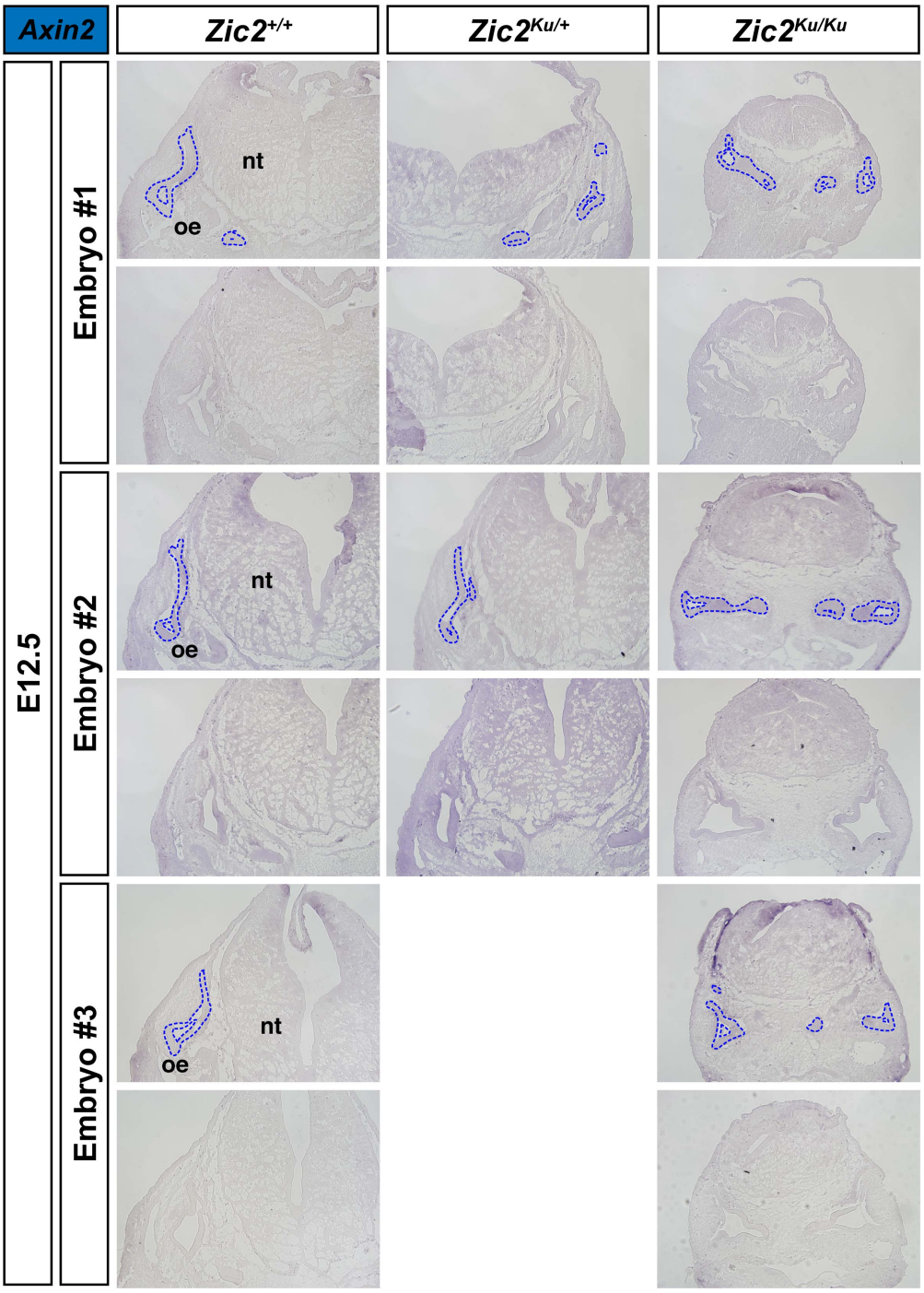

Figure A-19. *Axin2* expression in the otic region of *Zic2*$^{+/+}$, *Zic2*$^{Ku/+}$, and *Zic2*$^{Ku/Ku}$ mouse embryos at E12.5. *In situ* hybridization on 12µm transverse sections through the otocyst of E12.5 mouse embryos using a probe for *Axin2*. Abbreviations: oe, otic epithelium; nt, neural tube. Blue dashed line outlines the otic epithelium. Top and bottom sections within each embryo cluster ("embryo #1", "embryo #2", "embryo #3") are from different levels of the ear in the same embryo. **[n=3 for *Zic2*$^{+/+}$ and *Zic2*$^{Ku/Ku}$; n=2 for *Zic2*$^{Ku/+}$]**

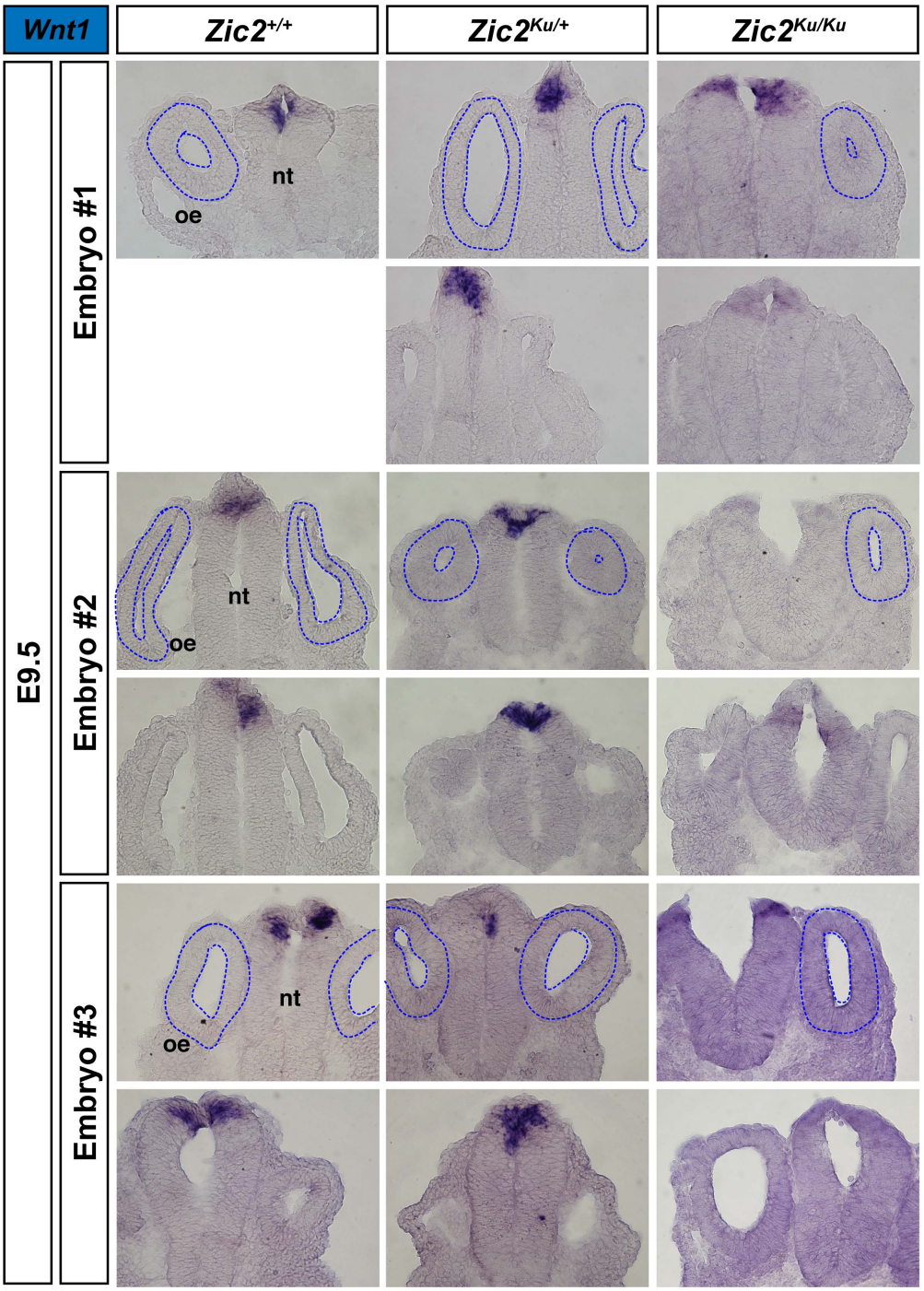

Figure A-20. *Wnt1* expression in the otic region of *Zic2*$^{+/+}$, *Zic2*$^{Ku/+}$, and *Zic2*$^{Ku/Ku}$ mouse embryos at E9.5. *In situ* hybridization on 12µm transverse sections through the otocyst of E9.5 mouse embryos using a probe for *Wnt1*. Abbreviations: oe, otic epithelium; nt, neural tube. Blue dashed line outlines the otic epithelium. Top and bottom sections within each embryo cluster ("embryo #1", "embryo #2", "embryo #3") are from different levels of the ear in the same embryo. **[n=3 for all genotypes]**

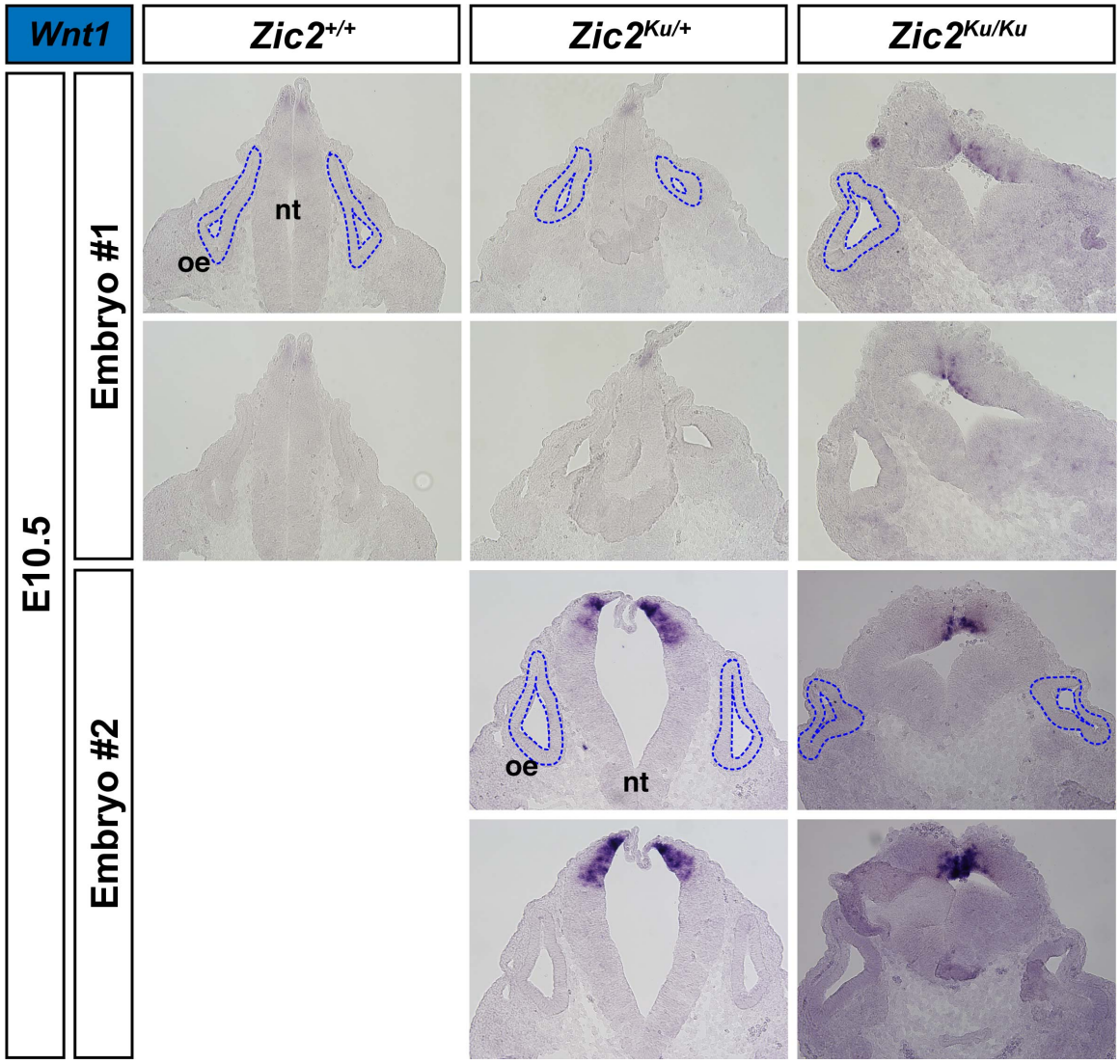

Figure A-21. *Wnt1* expression in the otic region of *Zic2*$^{+/+}$, *Zic2*$^{Ku/+}$, and *Zic2*$^{Ku/Ku}$ mouse embryos at E10.5. *In situ* hybridization on 12µm transverse sections through the otocyst of E10.5 mouse embryos using a probe for *Wnt1*. Abbreviations: oe, otic epithelium; nt, neural tube. Blue dashed line outlines the otic epithelium. Top and bottom sections within each embryo cluster ("embryo #1", "embryo #2") are from different levels of the ear in the same embryo. **[n=1 for *Zic2*$^{+/+}$; n=2 for *Zic2*$^{Ku/+}$ and *Zic2*$^{Ku/Ku}$]**

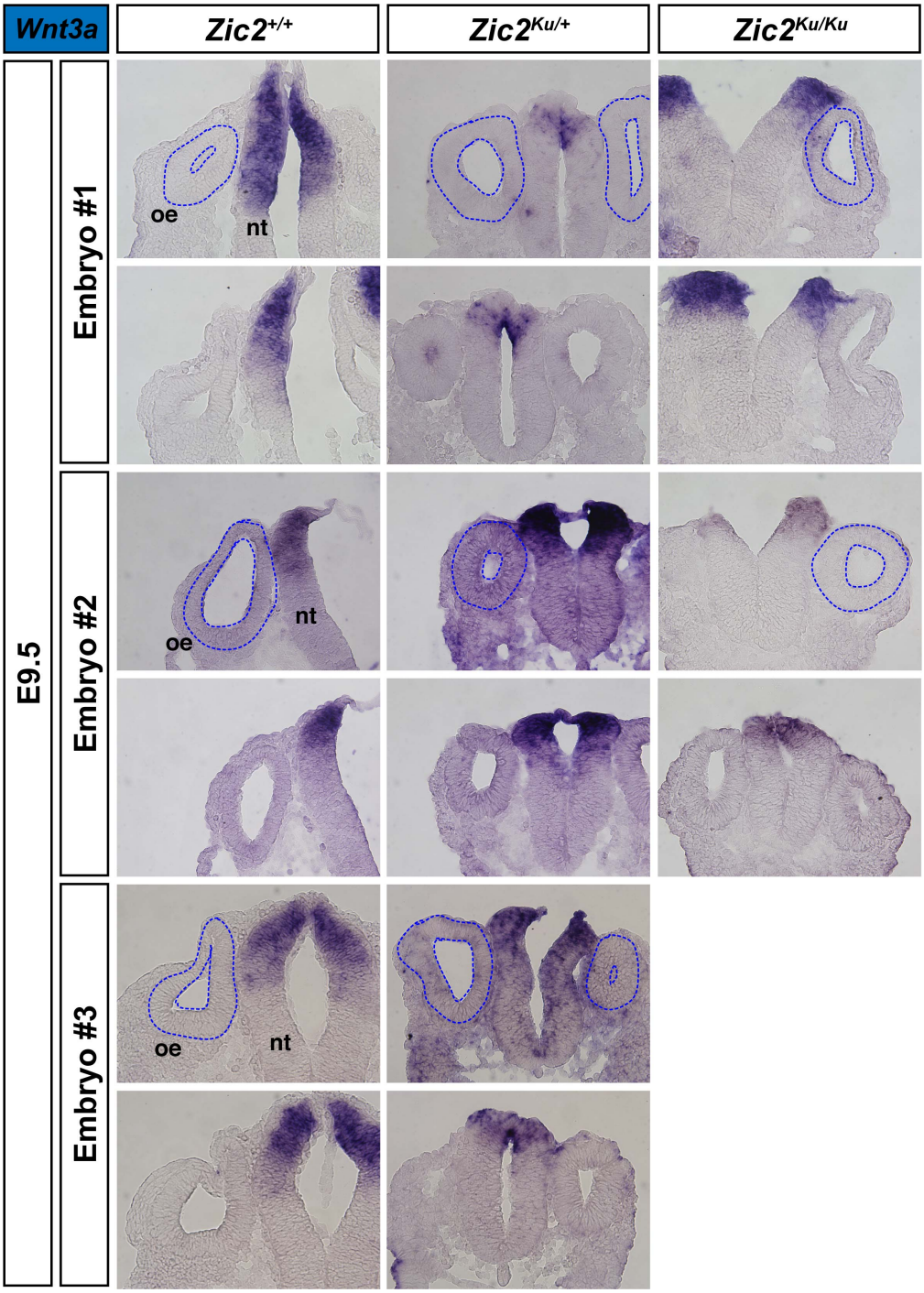

Figure A-22. *Wnt3a* expression in the otic region of *Zic2*$^{+/+}$, *Zic2*$^{Ku/+}$, and *Zic2*$^{Ku/Ku}$ mouse embryos at E9.5. *In situ* hybridization on 12µm transverse sections through the otocyst of E9.5 mouse embryos using a probe for *Wnt3a*. Abbreviations: oe, otic epithelium; nt, neural tube. Blue dashed line outlines the otic epithelium. Top and bottom sections within each embryo cluster ("embryo #1", "embryo #2", "embryo #3") are from different levels of the ear in the same embryo. **[n=3 for *Zic2*$^{+/+}$ and *Zic2*$^{Ku/+}$; n=2 for *Zic2*$^{Ku/Ku}$]**

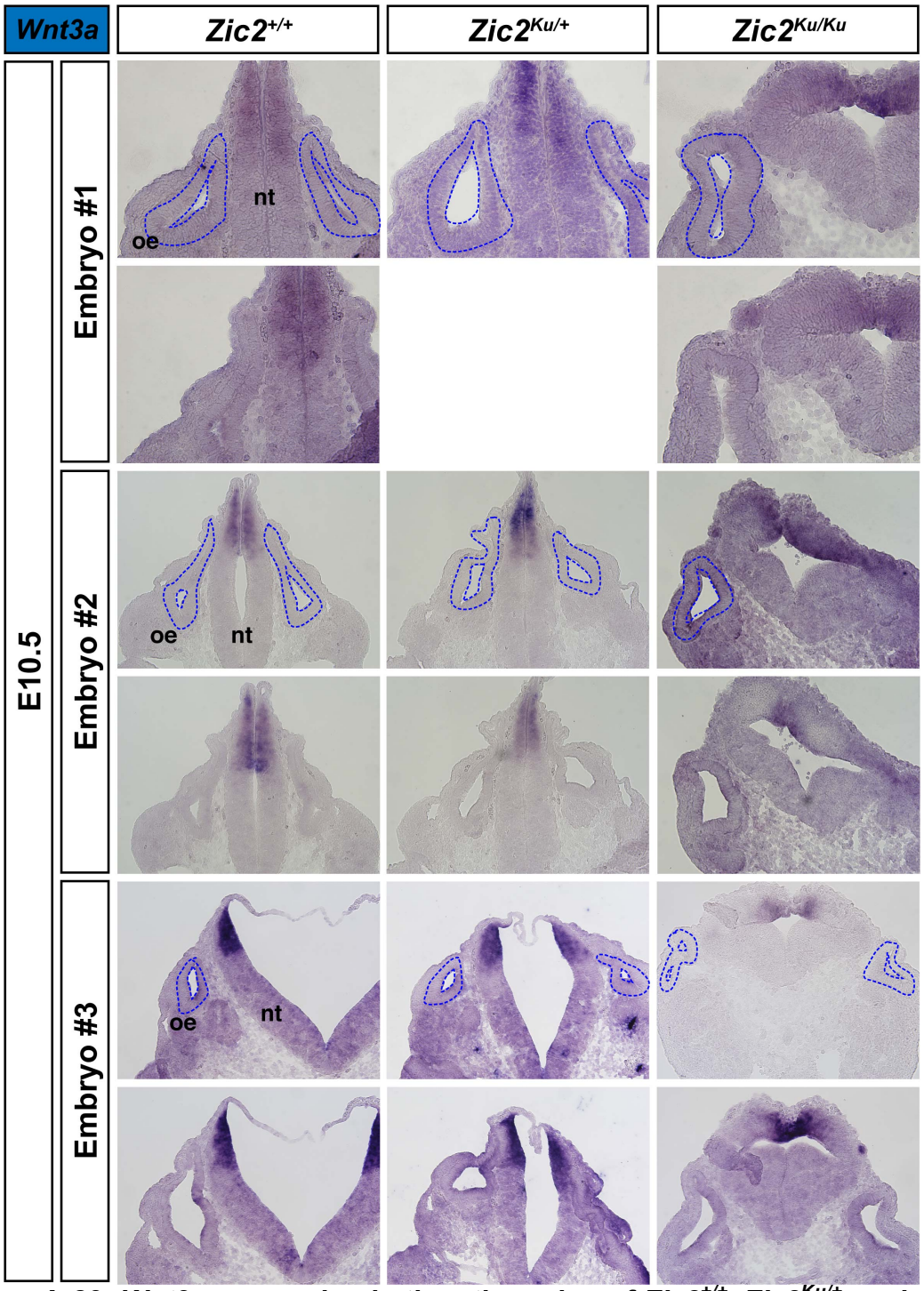

Figure A-23. *Wnt3a* expression in the otic region of *Zic2*$^{+/+}$, *Zic2*$^{Ku/+}$, and *Zic2*$^{Ku/Ku}$ mouse embryos at E10.5. *In situ* hybridization on 12µm transverse sections through the otocyst of E10.5 mouse embryos using a probe for *Wnt3a*. Abbreviations: oe, otic epithelium; nt, neural tube. Blue dashed line outlines the otic epithelium. Top and bottom sections within each embryo cluster ("embryo #1", "embryo #2", "embryo #3") are from different levels of the ear in the same embryo. **[n=3 for all genotypes]**

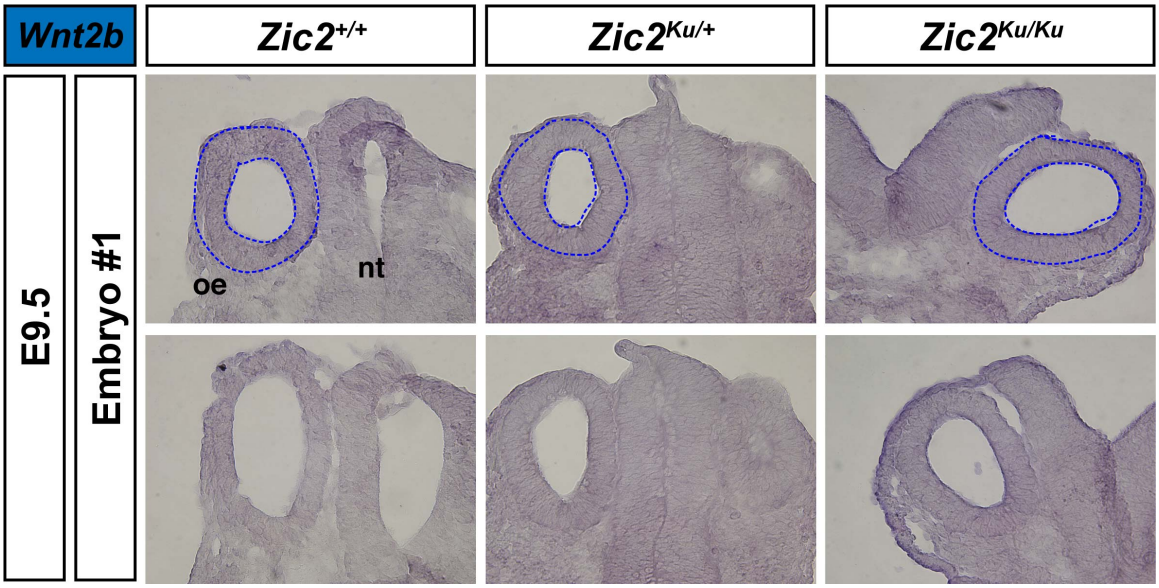

Figure A-24. *Wnt2b* expression in the otic region of *Zic2*$^{+/+}$, *Zic2*$^{Ku/+}$, and *Zic2*$^{Ku/Ku}$ mouse embryos at E9.5. *In situ* hybridization on 12µm transverse sections through the otocyst of E9.5 mouse embryos using a probe for *Wnt2b*. Abbreviations: oe, otic epithelium; nt, neural tube. Blue dashed line outlines the otic epithelium. Top and bottom sections within each embryo cluster ("embryo #1") are from different levels of the ear in the same embryo. **[n=1 for all genotypes]**

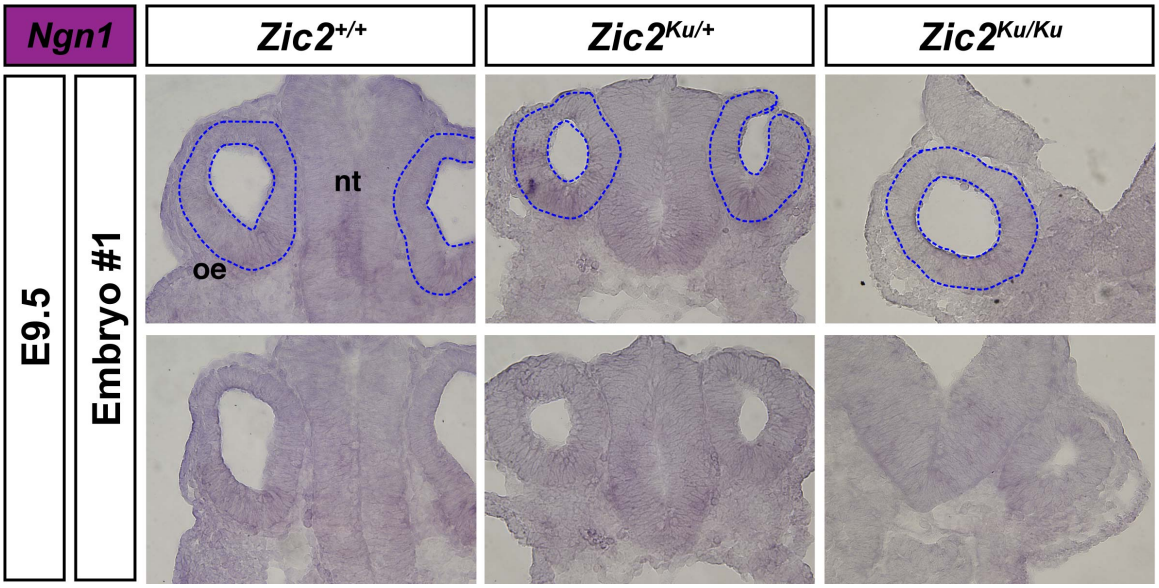

Figure A-25. *Ngn1* expression in the otic region of *Zic2*$^{+/+}$, *Zic2*$^{Ku/+}$, and *Zic2*$^{Ku/Ku}$ mouse embryos at E9.5. *In situ* hybridization on 12µm transverse sections through the otocyst of E9.5 mouse embryos using a probe for *Ngn1*. Abbreviations: oe, otic epithelium; nt, neural tube. Blue dashed line outlines the otic epithelium. Top and bottom sections within each embryo cluster ("embryo #1") are from different levels of the ear in the same embryo. **[n=1 for all genotypes]**

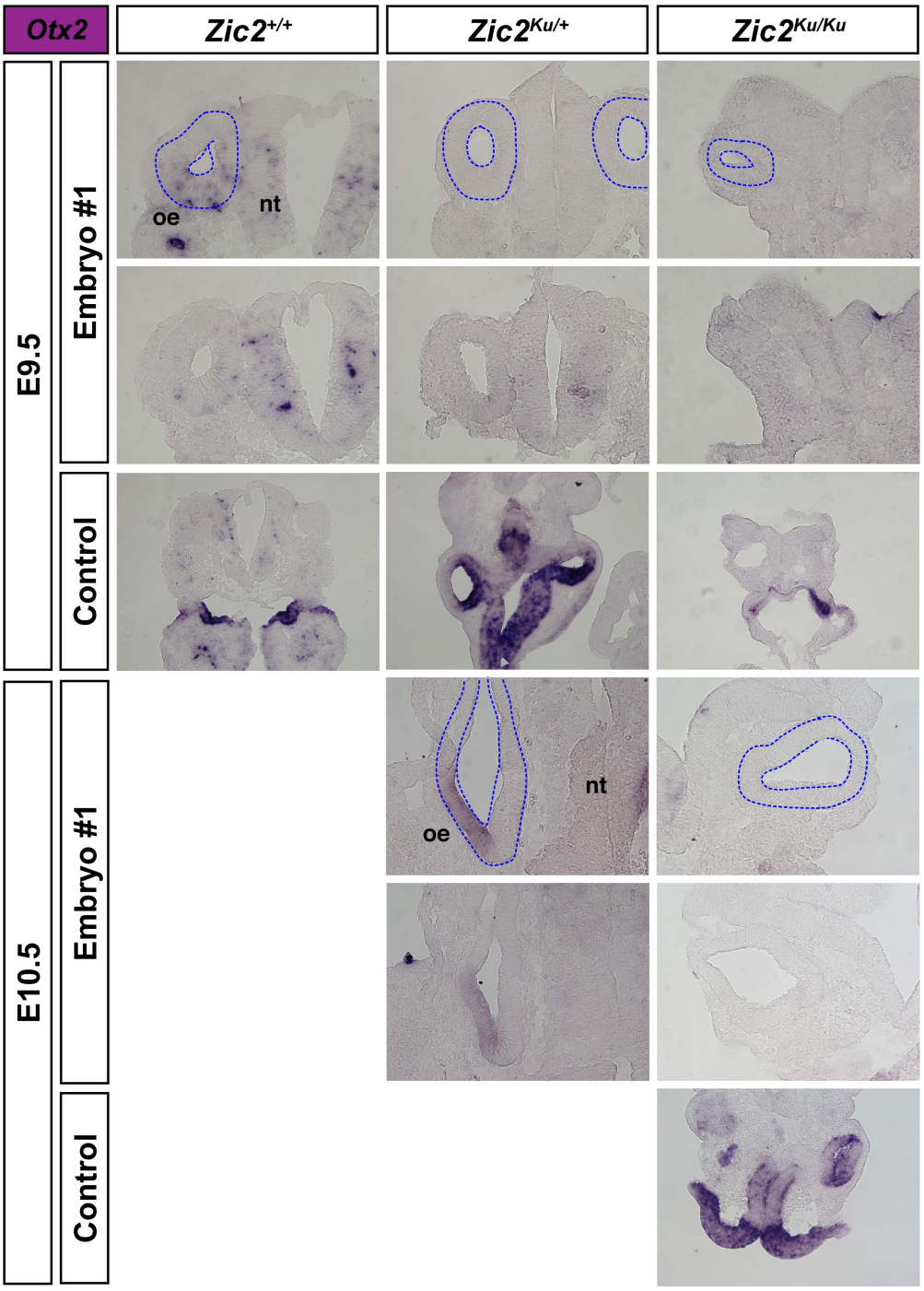

Figure A-26. *Otx2* expression in the otic region of *Zic2*$^{+/+}$, *Zic2*$^{Ku/+}$, and *Zic2*$^{Ku/Ku}$ mouse embryos at E9.5. and E10.5. *In situ* hybridization on 12µm transverse sections through the otocyst of E9.5 (top 3 rows) and E10.5 (bottom 3 rows) mouse embryos using a probe for *Otx2*. Abbreviations: oe, otic epithelium; nt, neural tube. Blue dashed line outlines the otic epithelium. Top and bottom sections within each embryo cluster ("embryo #1") are from different levels of the ear in the same embryo. **[E9.5: n=1 for all genotypes; E10.5: n=1 for *Zic2*$^{Ku/+}$ and *Zic2*$^{Ku/Ku}$]**

References

Acke, F. R., I. J. Dhooge, et al. (2012). "Hearing impairment in Stickler syndrome: a systematic review." Orphanet J Rare Dis **7**: 84.

Ali, R. G., H. M. Bellchambers, et al. (2012). "Zinc fingers of the cerebellum (Zic): transcription factors and co-factors." Int J Biochem Cell Biol **44**(11): 2065-2068.

Alsina, B., F. Giraldez, et al. (2009). "Patterning and cell fate in ear development." Int J Dev Biol **53**(8-10): 1503-1513.

Angelaki, D. E. and K. E. Cullen (2008). "Vestibular system: the many facets of a multimodal sense." Annu Rev Neurosci **31**: 125-150.

Appler, J. M. and L. V. Goodrich (2011). "Connecting the ear to the brain: Molecular mechanisms of auditory circuit assembly." Prog Neurobiol **93**(4): 488-508.

Arnold, J. S., E. M. Braunstein, et al. (2006). "Tissue-specific roles of Tbx1 in the development of the outer, middle and inner ear, defective in 22q11DS patients." Hum Mol Genet **15**(10): 1629-1639.

Aruga, J. (2004). "The role of Zic genes in neural development." Mol Cell Neurosci **26**(2): 205-221.

Aruga, J., T. Inoue, et al. (2002). "Zic2 controls cerebellar development in cooperation with Zic1." J Neurosci **22**(1): 218-225.

Aruga, J., A. Kamiya, et al. (2006). "A wide-range phylogenetic analysis of Zic proteins: implications for correlations between protein structure conservation and body plan complexity." Genomics **87**(6): 783-792.

Aruga, J., O. Minowa, et al. (1998). "Mouse Zic1 is involved in cerebellar development." J Neurosci **18**(1): 284-293.

Aruga, J., K. Mizugishi, et al. (1999). "Zic1 regulates the patterning of vertebral arches in cooperation with Gli3." Mech Dev **89**(1-2): 141-150.

Aruga, J., T. Nagai, et al. (1996). "The mouse zic gene family. Homologues of the Drosophila pair-rule gene odd-paired." J Biol Chem **271**(2): 1043-1047.

Aruga, J., N. Yokota, et al. (1994). "A novel zinc finger protein, zic, is involved in neurogenesis, especially in the cell lineage of cerebellar granule cells." J Neurochem **63**(5): 1880-1890.

Baker, K., D. E. Brough, et al. (2009). "Repair of the vestibular system via adenovector delivery of Atoh1: a potential treatment for balance disorders." Adv Otorhinolaryngol **66**: 52-63.

Bank, L. M., L. M. Bianchi, et al. (2012). "Macrophage migration inhibitory factor acts as a neurotrophin in the developing inner ear." Development **139**(24): 4666-4674.

Barald, K. F. and M. W. Kelley (2004). "From placode to polarization: new tunes in inner ear development." Development **131**(17): 4119-4130.

Bedard, J. E., J. D. Purnell, et al. (2007). "Nuclear import and export signals are essential for proper cellular trafficking and function of ZIC3." Hum Mol Genet **16**(2): 187-198.

Benedyk, M. J., J. R. Mullen, et al. (1994). "odd-paired: a zinc finger pair-rule protein required for the timely activation of engrailed and wingless in Drosophila embryos." Genes Dev **8**(1): 105-117.

Bermingham, N. A., B. A. Hassan, et al. (1999). "Math1: an essential gene for the generation of inner ear hair cells." Science **284**(5421): 1837-1841.

Bird, J. E., N. Daudet, et al. (2010). "Supporting cells eliminate dying sensory hair cells to maintain epithelial integrity in the avian inner ear." J Neurosci **30**(37): 12545-12556.

Blank, M. C., I. Grinberg, et al. (2011). "Multiple developmental programs are altered by loss of Zic1 and Zic4 to cause Dandy-Walker malformation cerebellar pathogenesis." Development **138**(6): 1207-1216.

Bok, J., M. Bronner-Fraser, et al. (2005). "Role of the hindbrain in dorsoventral but not anteroposterior axial specification of the inner ear." Development **132**(9): 2115-2124.

Bok, J., L. J. Brunet, et al. (2007). "Role of hindbrain in inner ear morphogenesis: analysis of Noggin knockout mice." Dev Biol **311**(1): 69-78.

Bok, J., W. Chang, et al. (2007). "Patterning and morphogenesis of the vertebrate inner ear." Int J Dev Biol **51**(6-7): 521-533.

Bok, J., D. K. Dolson, et al. (2007). "Opposing gradients of Gli repressor and activators mediate Shh signaling along the dorsoventral axis of the inner ear." Development **134**(9): 1713-1722.

Bok, J., S. Raft, et al. (2011). "Transient retinoic acid signaling confers anterior-posterior polarity to the inner ear." Proc Natl Acad Sci U S A **108**(1): 161-166.

Bonnet, C. and A. El-Amraoui (2012). "Usher syndrome (sensorineural deafness and retinitis pigmentosa): pathogenesis, molecular diagnosis and therapeutic approaches." Curr Opin Neurol **25**(1): 42-49.

Braunstein, E. M., E. B. Crenshaw, 3rd, et al. (2008). "Cooperative function of Tbx1 and Brn4 in the periotic mesenchyme is necessary for cochlea formation." J Assoc Res Otolaryngol **9**(1): 33-43.

Braunstein, E. M., D. C. Monks, et al. (2009). "Tbx1 and Brn4 regulate retinoic acid metabolic genes during cochlear morphogenesis." BMC Dev Biol **9**: 31.

Breuskin, I., M. Bodson, et al. (2009). "Sox10 promotes the survival of cochlear progenitors during the establishment of the organ of Corti." Dev Biol **335**(2): 327-339.

Brewster, R., J. Lee, et al. (1998). "Gli/Zic factors pattern the neural plate by defining domains of cell differentiation." Nature **393**(6685): 579-583.

Brigande, J. V., A. E. Kiernan, et al. (2000). "Molecular genetics of pattern formation in the inner ear: do compartment boundaries play a role?" Proc Natl Acad Sci U S A **97**(22): 11700-11706.

Bronner, M. E. (2012). "Formation and migration of neural crest cells in the vertebrate embryo." Histochem Cell Biol **138**(2): 179-186.

Brown, A. S. and D. J. Epstein (2011). "Otic ablation of smoothened reveals direct and indirect requirements for Hedgehog signaling in inner ear development." Development **138**(18): 3967-3976.

Brown, L. and S. Brown (2009). "Zic2 is expressed in pluripotent cells in the blastocyst and adult brain expression overlaps with makers of neurogenesis." Gene Expr Patterns **9**(1): 43-49.

Brown, L., M. Paraso, et al. (2005). "In vitro analysis of partial loss-of-function ZIC2 mutations in holoprosencephaly: alanine tract expansion modulates DNA binding and transactivation." Hum Mol Genet **14**(3): 411-420.

Brown, L. Y., S. Odent, et al. (2001). "Holoprosencephaly due to mutations in ZIC2: alanine tract expansion mutations may be caused by parental somatic recombination." Hum Mol Genet **10**(8): 791-796.

Brown, S. A., D. Warburton, et al. (1998). "Holoprosencephaly due to mutations in ZIC2, a homologue of Drosophila odd-paired." Nat Genet **20**(2): 180-183.

Burton, Q., L. K. Cole, et al. (2004). "The role of Pax2 in mouse inner ear development." Dev Biol **272**(1): 161-175.

Buttner-Ennever, J. A. (1999). "A review of otolith pathways to brainstem and cerebellum." Ann N Y Acad Sci **871**: 51-64.

Cadot, S., D. Frenz, et al. (2012). "A novel method for retinoic acid administration reveals differential and dose-dependent downregulation of Fgf3 in the developing inner ear and anterior CNS." Dev Dyn **241**(4): 741-758.

Carrel, T., S. M. Purandare, et al. (2000). "The X-linked mouse mutation Bent tail is associated with a deletion of the Zic3 locus." Hum Mol Genet **9**(13): 1937-1942.

Cervera-Paz, F. J. and M. J. Manrique (2007). "Auditory brainstem implants: past, present and future prospects." Acta Neurochir Suppl **97**(Pt 2): 437-442.

Chambers, D. and I. Mason (2000). "Expression of sprouty2 during early development of the chick embryo is coincident with known sites of FGF signalling." Mech Dev **91**(1-2): 361-364.

Chan, W. Y. and P. P. Tam (1988). "A morphological and experimental study of the mesencephalic neural crest cells in the mouse embryo using wheat germ agglutinin-gold conjugate as the cell marker." Development **102**(2): 427-442.

Chatterjee, S., P. Kraus, et al. (2010). "A symphony of inner ear developmental control genes." BMC Genet **11**: 68.

Chen, W., N. Jongkamonwiwat, et al. (2012). "Restoration of auditory evoked responses by human ES-cell-derived otic progenitors." Nature **490**(7419): 278-282.

Chervenak, A. P., I. Hakim, et al. (2013). "Spatiotemporal expression of Zic genes during vertebrate inner ear development." Dev Dyn.

Choi, B. Y., J. Muskett, et al. (2011). "Hereditary hearing loss with thyroid abnormalities." Adv Otorhinolaryngol **70**: 43-49.

Choo, D. (2007). "The role of the hindbrain in patterning of the otocyst." Dev Biol **308**(2): 257-265.

Colletti, V., R. V. Shannon, et al. (2009). "Progress in restoration of hearing with the auditory brainstem implant." Prog Brain Res **175**: 333-345.

Cotanche, D. A. and K. H. Lee (1994). "Regeneration of hair cells in the vestibulocochlear system of birds and mammals." Curr Opin Neurobiol **4**(4): 509-514.

Cotanche, D. A., K. H. Lee, et al. (1994). "Hair cell regeneration in the bird cochlea following noise damage or ototoxic drug damage." Anat Embryol (Berl) **189**(1): 1-18.

Das, R. M., N. J. Van Hateren, et al. (2006). "A robust system for RNA interference in the chicken using a modified microRNA operon." Dev Biol **294**(2): 554-563.

Daudet, N. and J. Lewis (2005). "Two contrasting roles for Notch activity in chick inner ear development: specification of prosensory patches and lateral inhibition of hair-cell differentiation." Development **132**(3): 541-551.

Declercq, J., P. Sheshadri, et al. (2013). "Zic3 Enhances the Generation of Mouse Induced Pluripotent Stem Cells." Stem Cells Dev.

Dominguez-Frutos, E., V. Vendrell, et al. (2009). "Tissue-specific requirements for FGF8 during early inner ear development." Mech Dev **126**(10): 873-881.

Ebert, P. J., J. R. Timmer, et al. (2003). "Zic1 represses Math1 expression via interactions with the Math1 enhancer and modulation of Math1 autoregulation." Development **130**(9): 1949-1959.

EBO. (2013). "Encyclopedia Brittanica Online." from http://www.britannica.com/.

Elms, P., P. Siggers, et al. (2003). "Zic2 is required for neural crest formation and hindbrain patterning during mouse development." Dev Biol **264**(2): 391-406.

EUCOMM. (2013). "International Mouse Knockout Consortium." from http://www.knockoutmouse.org/about/eucomm.

Freter, S., Y. Muta, et al. (2008). "Progressive restriction of otic fate: the role of FGF and Wnt in resolving inner ear potential." Development **135**(20): 3415-3424.

Friedman, T. B., J. M. Schultz, et al. (2011). "Usher syndrome: hearing loss with vision loss." Adv Otorhinolaryngol **70**: 56-65.

Fritzsch, B., N. Pan, et al. (2013). "Evolution and development of the tetrapod auditory system: an organ of Corti-centric perspective." Evol Dev **15**(1): 63-79.

Fujimi, T. J., M. Hatayama, et al. (2012). "Xenopus Zic3 controls notochord and organizer development through suppression of the Wnt/beta-catenin signaling pathway." Dev Biol **361**(2): 220-231.

Furushima, K., T. Murata, et al. (2005). "Characterization of Opr deficiency in mouse brain: subtle defects in dorsomedial telencephalon and medioventral forebrain." Dev Dyn **232**(4): 1056-1061.

Gebbia, M., G. B. Ferrero, et al. (1997). "X-linked situs abnormalities result from mutations in ZIC3." Nat Genet **17**(3): 305-308.

Gerlach-Bank, L. M., A. R. Cleveland, et al. (2004). "DAN directs endolymphatic sac and duct outgrowth in the avian inner ear." Dev Dyn **229**(2): 219-230.

Gong, T. W., A. D. Hegeman, et al. (1996). "Identification of genes expressed after noise exposure in the chick basilar papilla." Hear Res **96**(1-2): 20-32.

Grinberg, I. and K. J. Millen (2005). "The ZIC gene family in development and disease." Clin Genet **67**(4): 290-296.

Grinberg, I., H. Northrup, et al. (2004). "Heterozygous deletion of the linked genes ZIC1 and ZIC4 is involved in Dandy-Walker malformation." Nat Genet **36**(10): 1053-1055.

Groves, A. K. and M. Bronner-Fraser (2000). "Competence, specification and commitment in otic placode induction." Development **127**(16): 3489-3499.

Groves, A. K. and D. M. Fekete (2012). "Shaping sound in space: the regulation of inner ear patterning." Development **139**(2): 245-257.

Hamburger, V. and H. L. Hamilton (1992). "A series of normal stages in the development of the chick embryo. 1951." Dev Dyn **195**(4): 231-272.

Hatayama, M. and J. Aruga (2010). "Characterization of the tandem CWCH2 sequence motif: a hallmark of inter-zinc finger interactions." BMC Evol Biol **10**: 53.

Hatayama, M., T. Tomizawa, et al. (2008). "Functional and structural basis of the nuclear localization signal in the ZIC3 zinc finger domain." Hum Mol Genet **17**(22): 3459-3473.

Hawkins, R. D., S. Bashiardes, et al. (2007). "Large scale gene expression profiles of regenerating inner ear sensory epithelia." PLoS One **2**(6): e525.

Herman, G. E. and H. M. El-Hodiri (2002). "The role of ZIC3 in vertebrate development." Cytogenet Genome Res **99**(1-4): 229-235.

Hidalgo-Sanchez, M., R. Alvarado-Mallart, et al. (2000). "Pax2, Otx2, Gbx2 and Fgf8 expression in early otic vesicle development." Mech Dev **95**(1-2): 225-229.

Holmes, K. E., M. J. Wyatt, et al. (2011). "Direct delivery of MIF morpholinos into the zebrafish otocyst by injection and electroporation affects inner ear development." J Vis Exp(47).

Houtmeyers, R., J. Souopgui, et al. (2013). "The ZIC gene family encodes multi-functional proteins essential for patterning and morphogenesis." Cell Mol Life Sci.

Hu, Z. and M. Ulfendahl (2013). "The potential of stem cells for the restoration of auditory function in humans." Regen Med **8**(3): 309-318.

Hu, Z., M. Ulfendahl, et al. (2004). "Central migration of neuronal tissue and embryonic stem cells following transplantation along the adult auditory nerve." Brain Res **1026**(1): 68-73.

Hu, Z., D. Wei, et al. (2005). "Survival and neural differentiation of adult neural stem cells transplanted into the mature inner ear." Exp Cell Res **302**(1): 40-47.

Hutson, M. R., J. E. Lewis, et al. (1999). "Expression of Pax2 and patterning of the chick inner ear." J Neurocytol **28**(10-11): 795-807.

Inoue, T., M. Hatayama, et al. (2004). "Mouse Zic5 deficiency results in neural tube defects and hypoplasia of cephalic neural crest derivatives." Dev Biol **270**(1): 146-162.

Izumikawa, M., R. Minoda, et al. (2005). "Auditory hair cell replacement and hearing improvement by Atoh1 gene therapy in deaf mammals." Nat Med **11**(3): 271-276.

Jayasena, C. S., T. Ohyama, et al. (2008). "Notch signaling augments the canonical Wnt pathway to specify the size of the otic placode." Development **135**(13): 2251-2261.

Jeong, J. and A. P. McMahon (2005). "Growth and pattern of the mammalian neural tube are governed by partially overlapping feedback activities of the hedgehog antagonists patched 1 and Hhip1." Development **132**(1): 143-154.

Jho, E. H., T. Zhang, et al. (2002). "Wnt/beta-catenin/Tcf signaling induces the transcription of Axin2, a negative regulator of the signaling pathway." Mol Cell Biol **22**(4): 1172-1183.

Jung, J. Y., M. R. Avenarius, et al. (2013). "siRNA targeting Hes5 augments hair cell regeneration in aminoglycoside-damaged mouse utricle." Mol Ther **21**(4): 834-841.

Jungbluth, S., K. Willecke, et al. (2002). "Segment-specific expression of connexin31 in the embryonic hindbrain is regulated by Krox20." Dev Dyn **223**(4): 544-551.

Kalogeropoulos, M., S. S. Varanasi, et al. (2010). "Zic1 transcription factor in bone: neural developmental protein regulates mechanotransduction in osteocytes." FASEB J **24**(8): 2893-2903.

Karaman, A. and C. Aliagaoglu (2006). "Waardenburg syndrome type 1." Dermatol Online J **12**(3): 21.

Kawamoto, K., M. Izumikawa, et al. (2009). "Spontaneous hair cell regeneration in the mouse utricle following gentamicin ototoxicity." Hear Res **247**(1): 17-26.

Kelley, M. W. (2006). "Regulation of cell fate in the sensory epithelia of the inner ear." Nat Rev Neurosci **7**(11): 837-849.

Kiernan, A. E. (2006). "The paintfill method as a tool for analyzing the three-dimensional structure of the inner ear." Brain Res **1091**(1): 270-276.

Kil, S. H., A. Streit, et al. (2005). "Distinct roles for hindbrain and paraxial mesoderm in the induction and patterning of the inner ear revealed by a study of vitamin-A-deficient quail." Dev Biol **285**(1): 252-271.

Kimberling, W. J., N. Borsa, et al. (2011). "Hearing loss disorders associated with renal disease." Adv Otorhinolaryngol **70**: 75-83.

Klootwijk, R., B. Franke, et al. (2000). "A deletion encompassing Zic3 in bent tail, a mouse model for X-linked neural tube defects." Hum Mol Genet **9**(11): 1615-1622.

Kopecky, B. J., I. Jahan, et al. (2013). "Correct timing of proliferation and differentiation is necessary for normal inner ear development and auditory hair cell viability." Dev Dyn **242**(2): 132-147.

Koyabu, Y., K. Nakata, et al. (2001). "Physical and functional interactions between Zic and Gli proteins." J Biol Chem **276**(10): 6889-6892.

Krull, C. E. (2004). "A primer on using in ovo electroporation to analyze gene function." Dev Dyn **229**(3): 433-439.

Kuchta, J. (2007). "Twenty-five years of auditory brainstem implants: perspectives." Acta Neurochir Suppl **97**(Pt 2): 443-449.

Ladher, R. K., P. O'Neill, et al. (2010). "From shared lineage to distinct functions: the development of the inner ear and epibranchial placodes." Development **137**(11): 1777-1785.

Ladher, R. K., T. J. Wright, et al. (2005). "FGF8 initiates inner ear induction in chick and mouse." Genes Dev **19**(5): 603-613.

Lawoko-Kerali, G., M. N. Rivolta, et al. (2002). "Expression of the transcription factors GATA3 and Pax2 during development of the mammalian inner ear." J Comp Neurol **442**(4): 378-391.

Layden, M. J., N. P. Meyer, et al. (2010). "Expression and phylogenetic analysis of the zic gene family in the evolution and development of metazoans." Evodevo **1**(1): 12.

Lee, Y. S., F. Liu, et al. (2006). "A morphogenetic wave of p27Kip1 transcription directs cell cycle exit during organ of Corti development." Development **133**(15): 2817-2826.

Li, H., H. Liu, et al. (2004). "Correlation of Pax-2 expression with cell proliferation in the developing chicken inner ear." J Neurobiol **60**(1): 61-70.

Li, H., G. Roblin, et al. (2003). "Generation of hair cells by stepwise differentiation of embryonic stem cells." Proc Natl Acad Sci U S A **100**(23): 13495-13500.

Liang, J. K., J. Bok, et al. (2010). "Distinct contributions from the hindbrain and mesenchyme to inner ear morphogenesis." Dev Biol **337**(2): 324-334.

Lim, H. H., M. Lenarz, et al. (2009). "Auditory midbrain implant: a review." Trends Amplif **13**(3): 149-180.

Lim, L. S., F. H. Hong, et al. (2010). "The pluripotency regulator Zic3 is a direct activator of the Nanog promoter in ESCs." Stem Cells **28**(11): 1961-1969.

Lin, V., J. S. Golub, et al. (2011). "Inhibition of Notch activity promotes nonmitotic regeneration of hair cells in the adult mouse utricles." J Neurosci **31**(43): 15329-15339.

Ma, Q., Z. Chen, et al. (1998). "neurogenin1 is essential for the determination of neuronal precursors for proximal cranial sensory ganglia." Neuron **20**(3): 469-482.

Macatee, T. L., B. P. Hammond, et al. (2003). "Ablation of specific expression domains reveals discrete functions of ectoderm- and endoderm-derived FGF8 during cardiovascular and pharyngeal development." Development **130**(25): 6361-6374.

Mahmood, R., P. Kiefer, et al. (1995). "Multiple roles for FGF-3 during cranial neural development in the chicken." Development **121**(5): 1399-1410.

Masindova, I., L. Varga, et al. (2012). "Molecular and hereditary mechanisms of sensorineural hearing loss with focus on selected endocrinopathies." Endocr Regul **46**(3): 167-186.

Maurus, D. and W. A. Harris (2009). "Zic-associated holoprosencephaly: zebrafish Zic1 controls midline formation and forebrain patterning by regulating Nodal, Hedgehog, and retinoic acid signaling." Genes Dev **23**(12): 1461-1473.

McMahon, A. R. and C. S. Merzdorf (2010). "Expression of the zic1, zic2, zic3, and zic4 genes in early chick embryos." BMC Res Notes **3**: 167.

Merzdorf, C. S. (2007). "Emerging roles for zic genes in early development." Dev Dyn **236**(4): 922-940.

Merzdorf, C. S. and H. L. Sive (2006). "The zic1 gene is an activator of Wnt signaling." Int J Dev Biol **50**(7): 611-617.

Mizugishi, K., J. Aruga, et al. (2001). "Molecular properties of Zic proteins as transcriptional regulators and their relationship to GLI proteins." J Biol Chem **276**(3): 2180-2188.

Mizugishi, K., M. Hatayama, et al. (2004). "Myogenic repressor I-mfa interferes with the function of Zic family proteins." Biochem Biophys Res Commun **320**(1): 233-240.

Nagai, T., J. Aruga, et al. (2000). "Zic2 regulates the kinetics of neurulation." Proc Natl Acad Sci U S A **97**(4): 1618-1623.

Nakamura, H., T. Katahira, et al. (2004). "Gain- and loss-of-function in chick embryos by electroporation." Mech Dev **121**(9): 1137-1143.

NIDCD. (2013). "Health Info/Statistics and Epidemiology/Quick Statistics." 2013.

Nornes, H. O., G. R. Dressler, et al. (1990). "Spatially and temporally restricted expression of Pax2 during murine neurogenesis." Development **109**(4): 797-809.

Nusslein-Volhard, C. and E. Wieschaus (1980). "Mutations affecting segment number and polarity in Drosophila." Nature **287**(5785): 795-801.

Nyholm, M. K., S. F. Wu, et al. (2007). "The zebrafish zic2a-zic5 gene pair acts downstream of canonical Wnt signaling to control cell proliferation in the developing tectum." Development **134**(4): 735-746.

Oesterle, E. C. and E. W. Rubel (1996). "Hair cell generation in vestibular sensory receptor epithelia." Ann N Y Acad Sci **781**: 34-46.

Oesterle, E. C., T. T. Tsue, et al. (1993). "Hair-cell regeneration in organ cultures of the postnatal chicken inner ear." Hear Res **70**(1): 85-108.

Ohyama, T. and A. K. Groves (2004). "Generation of Pax2-Cre mice by modification of a Pax2 bacterial artificial chromosome." Genesis **38**(4): 195-199.

Ohyama, T., O. A. Mohamed, et al. (2006). "Wnt signals mediate a fate decision between otic placode and epidermis." Development **133**(5): 865-875.

Okano, T., S. Xuan, et al. (2011). "Insulin-like growth factor signaling regulates the timing of sensory cell differentiation in the mouse cochlea." J Neurosci **31**(49): 18104-18118.

Pan, H., M. K. Gustafsson, et al. (2011). "A role for Zic1 and Zic2 in Myf5 regulation and somite myogenesis." Dev Biol **351**(1): 120-127.

Phippard, D., A. Heydemann, et al. (1998). "Changes in the subcellular localization of the Brn4 gene product precede mesenchymal remodeling of the otic capsule." Hear Res **120**(1-2): 77-85.

Popper, A. N. and R. R. Fay (1993). "Sound detection and processing by fish: critical review and major research questions." Brain Behav Evol **41**(1): 14-38.

Pourebrahim, R., R. Houtmeyers, et al. (2011). "Transcription factor Zic2 inhibits Wnt/beta-catenin protein signaling." J Biol Chem **286**(43): 37732-37740.

Purandare, S. M., S. M. Ware, et al. (2002). "A complex syndrome of left-right axis, central nervous system and axial skeleton defects in Zic3 mutant mice." Development **129**(9): 2293-2302.

Puschel, A. W., M. Westerfield, et al. (1992). "Comparative analysis of Pax-2 protein distributions during neurulation in mice and zebrafish." Mech Dev **38**(3): 197-208.

Raft, S., S. Nowotschin, et al. (2004). "Suppression of neural fate and control of inner ear morphogenesis by Tbx1." Development **131**(8): 1801-1812.

Reyes, J. H., K. S. O'Shea, et al. (2008). "Glutamatergic neuronal differentiation of mouse embryonic stem cells after transient expression of neurogenin 1

and treatment with BDNF and GDNF: in vitro and in vivo studies." J Neurosci **28**(48): 12622-12631.

Riccomagno, M. M., L. Martinu, et al. (2002). "Specification of the mammalian cochlea is dependent on Sonic hedgehog." Genes Dev **16**(18): 2365-2378.

Riccomagno, M. M., S. Takada, et al. (2005). "Wnt-dependent regulation of inner ear morphogenesis is balanced by the opposing and supporting roles of Shh." Genes Dev **19**(13): 1612-1623.

Riley, B. B. and B. T. Phillips (2003). "Ringing in the new ear: resolution of cell interactions in otic development." Dev Biol **261**(2): 289-312.

Rinkwitz-Brandt, S., H. H. Arnold, et al. (1996). "Regionalized expression of Nkx5-1, Nkx5-2, Pax2 and sek genes during mouse inner ear development." Hear Res **99**(1-2): 129-138.

Rinkwitz-Brandt, S., M. Justus, et al. (1995). "Distinct temporal expression of mouse Nkx-5.1 and Nkx-5.2 homeobox genes during brain and ear development." Mech Dev **52**(2-3): 371-381.

Rivolta, M. N., H. Li, et al. (2006). "Generation of inner ear cell types from embryonic stem cells." Methods Mol Biol **330**: 71-92.

Rubel, E. W., L. A. Dew, et al. (1995). "Mammalian vestibular hair cell regeneration." Science **267**(5198): 701-707.

Rubel, E. W. and B. Fritzsch (2002). "Auditory system development: primary auditory neurons and their targets." Annu Rev Neurosci **25**: 51-101.

Rubel, E. W., E. C. Oesterle, et al. (1991). "Hair cell regeneration in the avian inner ear." Ciba Found Symp **160**: 77-96; discussion 96-102.

Rubel, E. W. and J. S. Stone (1996). "Stimulating hair cell regeneration: on a wing and a prayer." Nat Med **2**(10): 1082-1083.

Safieddine, S., A. El-Amraoui, et al. (2012). "The auditory hair cell ribbon synapse: from assembly to function." Annu Rev Neurosci **35**: 509-528.

Sakurada, T., K. Mima, et al. (2005). "Neuronal cell type-specific promoter of the alpha CaM kinase II gene is activated by Zic2, a Zic family zinc finger protein." Neurosci Res **53**(3): 323-330.

Salero, E., R. Perez-Sen, et al. (2001). "Transcription factors Zic1 and Zic2 bind and transactivate the apolipoprotein E gene promoter." J Biol Chem **276**(3): 1881-1888.

Sanchez-Calderon, H., G. Martin-Partido, et al. (2002). "Differential expression of Otx2, Gbx2, Pax2, and Fgf8 in the developing vestibular and auditory sensory organs." Brain Res Bull **57**(3-4): 321-323.

Sanchez-Calderon, H., G. Martin-Partido, et al. (2005). "Pax2 expression patterns in the developing chick inner ear." Gene Expr Patterns **5**(6): 763-773.

Sanek, N. A., A. A. Taylor, et al. (2009). "Zebrafish zic2a patterns the forebrain through modulation of Hedgehog-activated gene expression." Development **136**(22): 3791-3800.

Saul, S. M., J. A. t. Brzezinski, et al. (2008). "Math5 expression and function in the central auditory system." Mol Cell Neurosci **37**(1): 153-169.

Scaal, M., J. Gros, et al. (2004). "In ovo electroporation of avian somites." Dev Dyn **229**(3): 643-650.

Schacht, J., A. E. Talaska, et al. (2012). "Cisplatin and aminoglycoside antibiotics: hearing loss and its prevention." Anat Rec (Hoboken) **295**(11): 1837-1850.

Scheich, H. (1991). "Auditory cortex: comparative aspects of maps and plasticity." Curr Opin Neurobiol **1**(2): 236-247.

Schlecker, C., M. Praetorius, et al. (2011). "Selective atonal gene delivery improves balance function in a mouse model of vestibular disease." Gene Ther **18**(9): 884-890.

Schwartz, M. S., S. R. Otto, et al. (2008). "Auditory brainstem implants." Neurotherapeutics **5**(1): 128-136.

Sechrist, J., G. N. Serbedzija, et al. (1993). "Segmental migration of the hindbrain neural crest does not arise from its segmental generation." Development **118**(3): 691-703.

Sennaroglu, L. and I. Ziyal (2012). "Auditory brainstem implantation." Auris Nasus Larynx **39**(5): 439-450.

Serbedzija, G. N., M. Bronner-Fraser, et al. (1992). "Vital dye analysis of cranial neural crest cell migration in the mouse embryo." Development **116**(2): 297-307.

Shen, Y. C., D. L. Thompson, et al. (2012). "The cytokine macrophage migration inhibitory factor (MIF) acts as a neurotrophin in the developing inner ear of the zebrafish, Danio rerio." Dev Biol **363**(1): 84-94.

Simkin, J. E., S. J. McKeown, et al. (2009). "Focal electroporation in ovo." Dev Dyn **238**(12): 3152-3155.

Staecker, H., M. Praetorius, et al. (2007). "Vestibular hair cell regeneration and restoration of balance function induced by math1 gene transfer." Otol Neurotol **28**(2): 223-231.

Stone, J. S. and D. A. Cotanche (1992). "Synchronization of hair cell regeneration in the chick cochlea following noise damage." J Cell Sci **102 (Pt 4)**: 671-680.

Stone, J. S. and D. A. Cotanche (2007). "Hair cell regeneration in the avian auditory epithelium." Int J Dev Biol **51**(6-7): 633-647.

Stone, J. S., S. G. Leano, et al. (1996). "Hair cell differentiation in chick cochlear epithelium after aminoglycoside toxicity: in vivo and in vitro observations." J Neurosci **16**(19): 6157-6174.

Stone, J. S., E. C. Oesterle, et al. (1998). "Recent insights into regeneration of auditory and vestibular hair cells." Curr Opin Neurol **11**(1): 17-24.

Sun Rhodes, L. S. and C. S. Merzdorf (2006). "The zic1 gene is expressed in chick somites but not in migratory neural crest." Gene Expr Patterns **6**(5): 539-545.

Sutherland, M. J., S. Wang, et al. (2013). "Zic3 is required in the migrating primitive streak for node morphogenesis and left-right patterning." Hum Mol Genet **22**(10): 1913-1923.

Thompson, D. L., L. M. Gerlach-Bank, et al. (2003). "Retinoic acid repression of bone morphogenetic protein 4 in inner ear development." Mol Cell Biol **23**(7): 2277-2286.

Torres, M. and F. Giraldez (1998). "The development of the vertebrate inner ear." Mech Dev **71**(1-2): 5-21.

Tosney, K. W. (1982). "The segregation and early migration of cranial neural crest cells in the avian embryo." Dev Biol **89**(1): 13-24.

Trainor, P. A., D. Sobieszczuk, et al. (2002). "Signalling between the hindbrain and paraxial tissues dictates neural crest migration pathways." Development **129**(2): 433-442.

Trowe, M. O., S. Shah, et al. (2010). "Loss of Sox9 in the periotic mesenchyme affects mesenchymal expansion and differentiation, and epithelial morphogenesis during cochlea development in the mouse." Dev Biol **342**(1): 51-62.

Tsue, T. T., E. C. Oesterle, et al. (1994). "Hair cell regeneration in the inner ear." Otolaryngol Head Neck Surg **111**(3 Pt 1): 281-301.

Urness, L. D., C. Li, et al. (2008). "Expression of ERK signaling inhibitors Dusp6, Dusp7, and Dusp9 during mouse ear development." Dev Dyn **237**(1): 163-169.

Vazquez-Echeverria, C., E. Dominguez-Frutos, et al. (2008). "Analysis of mouse kreisler mutants reveals new roles of hindbrain-derived signals in the establishment of the otic neurogenic domain." Dev Biol **322**(1): 167-178.

Vendrell, V., E. Carnicero, et al. (2000). "Induction of inner ear fate by FGF3." Development **127**(10): 2011-2019.

Vitelli, F., A. Viola, et al. (2003). "TBX1 is required for inner ear morphogenesis." Hum Mol Genet **12**(16): 2041-2048.

Volandri, G., F. Di Puccio, et al. (2011). "Biomechanics of the tympanic membrane." J Biomech **44**(7): 1219-1236.

Walsh, R. M., C. M. Hackney, et al. (2000). "Regeneration of the mammalian vestibular sensory epithelium following gentamicin-induced damage." J Otolaryngol **29**(6): 351-360.

Warchol, M. E., P. R. Lambert, et al. (1993). "Regenerative proliferation in inner ear sensory epithelia from adult guinea pigs and humans." Science **259**(5101): 1619-1622.

Ware, S. M., J. Peng, et al. (2004). "Identification and functional analysis of ZIC3 mutations in heterotaxy and related congenital heart defects." Am J Hum Genet **74**(1): 93-105.

Warner, S. J., M. R. Hutson, et al. (2003). "Expression of ZIC genes in the development of the chick inner ear and nervous system." Dev Dyn **226**(4): 702-712.

Warr, N., N. Powles-Glover, et al. (2008). "Zic2-associated holoprosencephaly is caused by a transient defect in the organizer region during gastrulation." Hum Mol Genet **17**(19): 2986-2996.

Watabe, Y., Y. Baba, et al. (2011). "The role of Zic family zinc finger transcription factors in the proliferation and differentiation of retinal progenitor cells." Biochem Biophys Res Commun **415**(1): 42-47.

Watanabe, K., K. Takeda, et al. (2000). "Expression of the Sox10 gene during mouse inner ear development." Brain Res Mol Brain Res **84**(1-2): 141-145.

Wessels, M. W., B. Kuchinka, et al. (2010). "Polyalanine expansion in the ZIC3 gene leading to X-linked heterotaxy with VACTERL association: a new polyalanine disorder?" J Med Genet **47**(5): 351-355.

Whitfield, T. T. and K. L. Hammond (2007). "Axial patterning in the developing vertebrate inner ear." Int J Dev Biol **51**(6-7): 507-520.

Wilkinson, D. G. and M. A. Nieto (1993). "Detection of messenger RNA by in situ hybridization to tissue sections and whole mounts." Methods Enzymol **225**: 361-373.

Wright, T. J. and S. L. Mansour (2003). "Fgf3 and Fgf10 are required for mouse otic placode induction." Development **130**(15): 3379-3390.

Xu, J. C., D. L. Huang, et al. (2012). "Type I hair cell regeneration induced by Math1 gene transfer following neomycin ototoxicity in rat vestibular sensory epithelium." Acta Otolaryngol **132**(8): 819-828.

Yang, S. M., W. Chen, et al. (2012). "Regeneration of stereocilia of hair cells by forced Atoh1 expression in the adult mammalian cochlea." PLoS One **7**(9): e46355.

Yang, Y., C. K. Hwang, et al. (2000). "ZIC2 and Sp3 repress Sp1-induced activation of the human D1A dopamine receptor gene." J Biol Chem **275**(49): 38863-38869.

Zelarayan, L. C., V. Vendrell, et al. (2007). "Differential requirements for FGF3, FGF8 and FGF10 during inner ear development." Dev Biol **308**(2): 379-391.

Zhang, P. Z., Y. He, et al. (2013). "Stem cell transplantation via the cochlear lateral wall for replacement of degenerated spiral ganglion neurons." Hear Res **298**: 1-9.

Zhang, Y. and L. Niswander (2013). "Zic2 is required for enteric nervous system development and neurite outgrowth: a mouse model of enteric hyperplasia and dysplasia." Neurogastroenterol Motil **25**(6): 538-541.

Zheng, J. L. and W. Q. Gao (2000). "Overexpression of Math1 induces robust production of extra hair cells in postnatal rat inner ears." Nat Neurosci **3**(6): 580-586.